UNIVERSITA' DEGLI STUDI DI FOGGIA

PhD Course

"Experimental and Regenerative Medicine"

XXXI Cycle

A novel biomarker for cancer and autoimmune diseases:

IGFBP6

Tutor

Prof. Arcangelo Liso

PhD Student

Dr. Rosa Trotta

Supervisor

Prof. Nazzareno Capitanio

Summary

Abbreviation

APC	antigen presenting cell
ARG1	arginase 1
ARMS	alveolar rhabdomyosarcoma
β-cat	beta-catenin
BC	breast cancer
BM	bone marrow
BMP	bone morphogenetic protein
CACO2	heterogeneous human epithelial colorectal adenocarcinoma cell line
CAD	coronary artery disease
CNS	central nervous system
CTL	cytotoxic T lymphocyte
DC	dendritic cell
DC-LAMP	DC-lysosome-associated membrane protein
DM	diabetes mellitus
Dsh	dishevelled
dsRNA	double-stranded RNA
ELISA	Enzyme-linked immunosorbent assay
ERMS	embryonal rhabdomyosarcoma
fMLP	*N*-formyl-methionyl-leucyl-phenylalanine
Fzd	frizzled
GBM	glioblastoma
GM-CSF	granulocyte-macrophage colony-stimulating factor
GSK3	glycogensynthase kinase 3
HAEC	human aortic endothelial cells
HCT116	human colon cancer cell line
HD	healthy donors
HK2	human renal tubular cancer cell lines
HSP	heat shock protein
HTN	hypertension
IFN	interferon
IGF	insulin-like growth factor
IGFBP	IGF binding protein
IL	interleukin
iNOS	nitric oxide synthase
LEF	lymphoid enhancer factor
LMP-1	LIM mineralization protein-1
LN	lymph node
LPS	lipopolysaccaride

LRP	low-density lipoprotein-related protein receptors
MANF	mesencephalic astrocyte-derived neurotrophic factor
MAP kinase	mitogen activated protein kinase
MCF-7 Cells	human breast adenocarcinoma cell line
MCP-1	monocyte chemoattractant protein-1
MDSC	myeloid-derived suppressor cells
MHC-I	major histocompatibility class I
MHC-II	major histocompatibility class II
MMP-9	metalloproteinase-9
moAb	monoclonal antibody
moDC	monocyte-derived dendritic cell
MPO	myeloperoxidase
$mtCa^{2+}$	mitochondrial calcium
NK	natural killer cells
NPC	nasopharyngeal carcinoma
OA	osteoarthritis
OC	ovarian cancer
OxPhos	oxidative phosphorylation
PC3	human prostate cancer cell line
Phb2	prohibitin-2
PLAT	tissue-type plasminogen activator
PLT	primary lymphoid tissue
PMA	phorbol 12-myristate 13-acetate
PRR	pathogen recognition receptor
RA	rheumatoid arthritis
RMS	rhabdomyosarcoma
ROI	reactive oxygen intermediates
RONS	reactive nitrogen and oxygen species
ROS	reactive oxygen species
RP	retinopathy
SL	synovial fluid
SLO	secondary lymphoid organ
ST	synovial tissue
T1DM	type 1 diabetes mellitus
T2DM	type 2 diabetes mellitus
TAN	tumor-associated neutrophil
TCF	T-cell factor
TD	thoracic duct
TGF	transforming growth factor
TLR 2/4	toll-like receptor 2/4

TMZ	temozolomide
TNF-α	tumor necrosis factor-alpha
TRα	thyroid hormone receptor-α1
VDR	vitamin D receptor

1. Introduction

Fever response is a characteristic symptom of infection and inflammatory disease retained through hundreds of millions of years of natural selection; is a hallmark of infection and inflammatory disease and has been shaped through hundreds of millions of years of natural selection [1]. The increase from 1 to 4°C of body temperature in endothermic (warm-blooded) animals is associated with improved survival and resolution of many infections [2]. The American College of Critical Care Medicine and the Infectious Diseases Society of America has defined fever as a body temperature of at least 38.3°C (101°F) [3, 4]. During infection, ecthotermic vertebrates can increase their body temperature through behavioral regulation [1], while, in the endothermic animals, the induction and the maintenance of fever involves numerous coordinated interplay between the innate immune system and neuronal circuits both in the central and peripheral nervous systems. Immune sensing of infection begins with the cell populations of innate immunity (macrophages, neutrophils and dendritic cells), which, through the pathogen recognition receptors (PRRs), stimulate the synthesis of pyrogenic cytokines, such as, IL-1, TNF-α and IL-6 both at the site of infection and within the brain [5, 6]. IL-6 and IL-1, in the hypothalamus, induce the synthesis of cyclooxygenase 2 (COX2) in the brain vascular endothelial cells with a consequent production of prostaglandin E2 (PGE2) by oxidizing arachidonic acid [7, 8]. PGE2 is considered the most important pyrogenic mediator of fever [9-11]. Thus, PGE2 can bind to the EP3 prostaglandin receptors expressed by thermoregulatory neurons in the median preoptic nucleus inside the hypothalamus [12], determining the release of norepinephrine (also known as noradrenaline) which raises body temperature by increasing the thermogenesis in brown adipose tissue, induces vasoconstriction in order to prevent passive heat loss [1, 13, 14] and acetylcholine which stimulates the muscles to convert the stored chemical energy into thermal energy increasing the overall metabolic rates [15]. Moreover, acetylcholine contributes to fever by stimulating muscle myocytes to induce shivering (**Figure 1**).

One benefit widely attributed to fever is the enhancement of immune-protective mechanisms following infection.

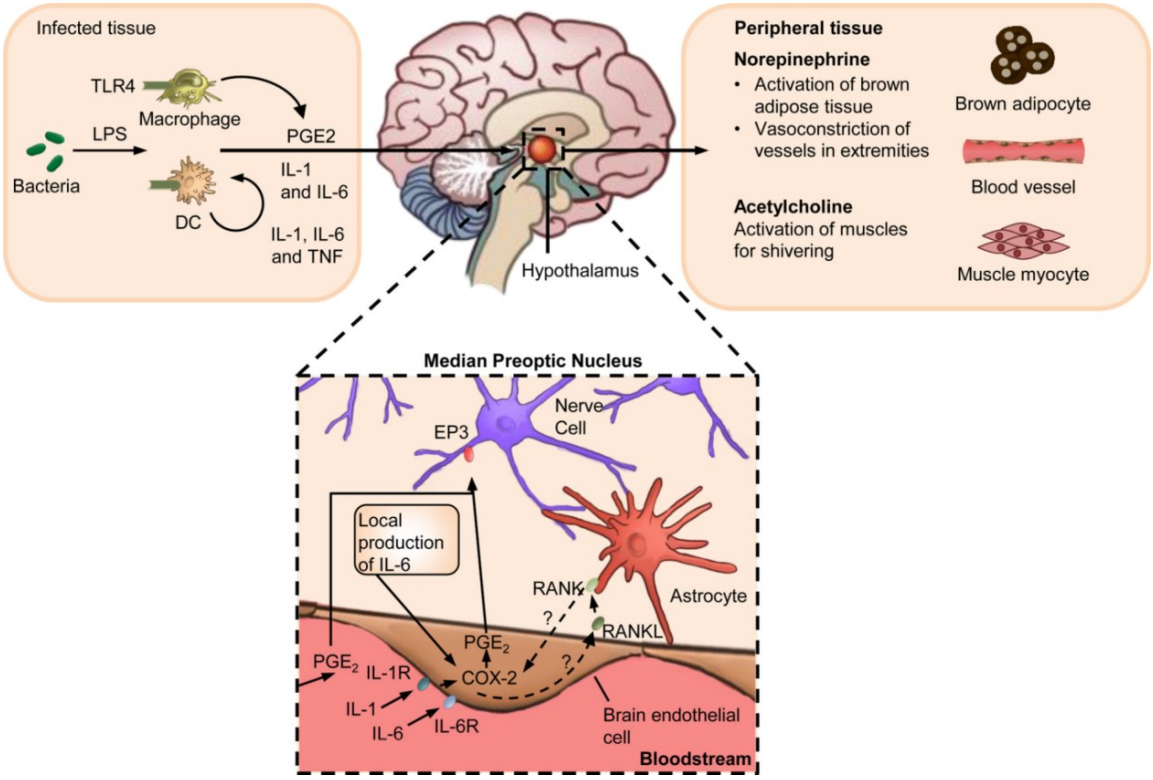

Figure 1. Induction of fever during infection ***(Evans, S.S. et al., 2015)***

Defence against pathogens involves tight spatial and temporal regulation of the immune system, and the pyrogenic cytokines that are produced during the induction of fever also operate locally to orchestrate immunity within infected tissues [16]. Some possible noninfectious causes of fever include blood transfusions, endocrine disturbances, alteration of oral mucosa leading mucositis, surgery and tumor fever [17-19]. Moreover, about 15-20% of patients with cancer have fever of unknown origin (FUO) [19], known as neoplastic fever or tumor fever. Unlike infectious fevers that tend to present with warmth, diaphoresis and chills reflective of peripheral vasodilation, neoplastic fever is commonly associated with diaphoresis and rubor and in some cases chills/rigors [20]. Many agents can induce fever, among them, antimicrobials, anticonvulsants, bisphosphonates, immunosuppressants, and antineoplastic agents. These agents are among the most common to induce fevers and are also frequently used in patients with cancer. Some examples are represented by: bleomycin, chlorambucil, cisplatin, daunorubicin, hydroxyurea, vincristine, and 6-mercaptupurine [21].

Several studies have shown that fever-like temperature changes might activate innate and also adaptive immunity [22, 23]. It is well-known that hypertermia can modulate the activities of immune cells, including dendritic cells [24] (innovative approach capable of enhancing the anti-tumor functions of DCs) and neutrophils [25]. Moreover, fever enhances DC cross-presenting functions by increasing DCs expression of MHC class I and class II molecules and co-stimulatory molecules, like CD80 and CD86, and stimulates the secretion of the IL-12 and TNF [26].

2. Dendritic cells, immunity and cancer

Dendritic cells (DCs) are the most potent professional Antigen-Presenting cells (APCs) *in* vivo. They are key regulators of the adaptive immune response, and play a fundamental role for T cell-mediated cancer immunity. However, numerous studies have concluded that DCs can infiltrate tumors.

DCs can be distinguished in different subsets: conventional dendritic cells (also known as classic dendritic cells, cDCs), plasmocytoid dendritic cells (pDCs), Langerhans cells and monocyte-derived dendritic cells (moDCs).

cDCs transport tumor antigens to draining lymph nodes and cross-present antigen to activate cytotoxic T lymphocytes [27]. These cells are very adept at initiating a T-cell response, directing T cell polarization, and presenting exogenous and endogenous Ag in both MHC-I and -II contexts. cDCs can respond to stimulation by pathogen associated signatures (PAMPs) by secreting large amounts of IFN-I (notably IFN-α and IFN-β) [28]. These cells are present in the thymus, spleen, and lymph nodes can be divided into two main subsets that are distinguished by the paths they follow to access the lymphoid organs [29].

pDCs are found circulating in the blood and in peripheral organs and show a characteristic surface phenotype and morphology. They are found in small numbers throughout the periphery and are recognized by their expression of B220, Ly6C, and PDCA. They were first identified in humans [30] and later in mice [31]. pDCs selectively express TLR7 and TLR9, generate high amounts of type I interferon (IFN-I) [32] and acquire the typical DC morphology after activation. Their activation and IFN-I production are fundamental for the initiation of antiviral immune responses. Thanks to the expression of MHC-II and co-stimulatory molecules, the pDCs also have the potential to act as antigen-presenting cells.

A substantial portion of DCs in the epidermal skin layer are a specialized subset of cells namely Langerhans cells. These cells have been described in many species of mammal.

After inflammation or infection, lymphoid and non-lymphoid organs can receive DCs that originate from monocyte infiltrates [33] and have been defined "monocyte-derived DCs" (moDCs) or "inflammatory DCs" (iDCs) [34, 35].

moDCs are phenotypically difficult to distinguish from cDCs because they share similar expression patterns of MHC-II, CD11b and CD11c; although, as the

monocytes from which they derive express CD64, the Fc-gamma receptor 1 (FcgRI) [36, 37]. In 1994, Sallusto and Lanzavecchia developed a protocol in order to generate dendritic cells in *vitro*, starting from monocytes stimulated with GM-CSF (Csf2) and IL-4 [38].

2.1 Dendritic cells activation

DCs can be activated by different molecules, such as, CD40, TNF-R and IL-1R. These molecules have been shown to activate transition from immature Ag-capturing cells to mature Ag-presenting DCs [39]. DCs maturation is a multistep process, which begins in the periphery after Ag encounter and/or inflammatory cytokines and completing during DC-T cell interaction. This process can be induced and/or regulated by numerous factors (**Figure 2**), including i) pathogen-related molecules such as lipopolysaccaride (LPS) [40], bacterial DNA [41-43] and dsRNA [44]; ii) in the local microenvironment, the balance between proinflammatory and anti-inflammatory signals, including TNF, IL-1, IL-6, IL-10, TGF-β and prostaglandins; and (iii) T cell-derived signals. The maturation is associated with numerous events, including i) loss of endocytic/phagocytic receptors; ii) up-regulation of costimulatory molecules (CD40, CD58, CD80 and CD86); iii) morphological changes with loss of adhesive structures, cytoskeleton reorganization (that can be controlled by actin-bundling protein p55 fascin [45]), and acquisition of high cell motility [46]; iv) shift in lysosomal compartments with CD68 down-regulation and DC-lysosome-associated membrane protein up-regulation (DC-LAMP); and v) modification of the MHC-II compartments.

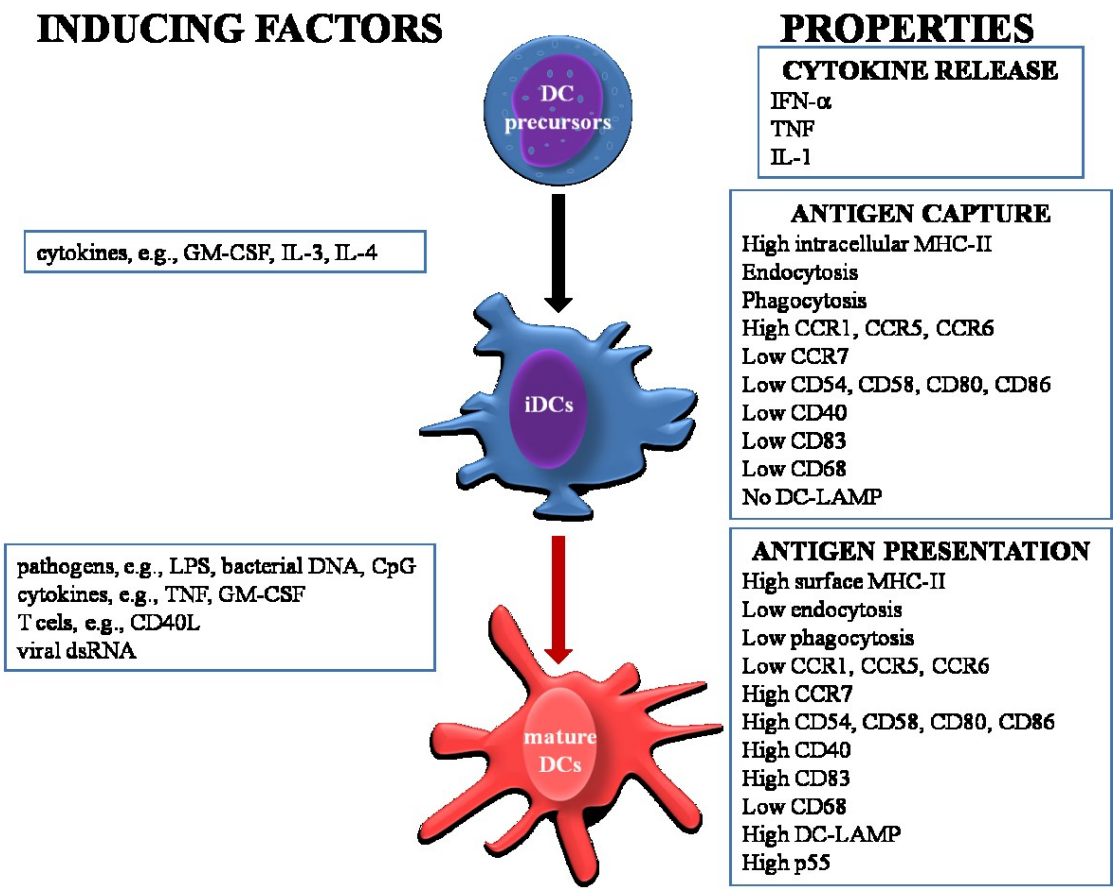

Figure 2. Maturation of Dendritic cells

2.2 Dendritic cells migration

DCs develop from precursors that originate from primary lymphoid tissues (PLT). Fully differentiated DCs are found in healthy tissues as immature cells, that is, endowed with highly-active endocytic machinery for sampling foreign Antigens but have not acquired the ability for priming of naive T cells [39]. DCs are very present in some tissues, such as, skin and mucosal surfaces because a central function of DCs in non-lymphoid tissues is the transport and presentation of antigenic cargo into and within secondary lymphoid organs (SLOs). The microarchitecture of secondary lymphoid tissues allows interactions between DCs, B cells and T cells that generate antigen in order to initiate adaptive immune responses [47]. The SLOs function is exercised thanks to the capacity of DCs to enter the small lymphatic vessels in the peripheral tissues and migrate to local draining lymph nodes (LNs). During the migration to the LN these Ag-bearing DCs mature, i.e. they assume an immunostimulatory phenotype. The maturation is coupled with the increased expression of the MHC complexes, the up-regulation of the co-stimulatory molecules and cytokines necessary for T cell priming. A small number of cells that have migrated to the lymphatic system are not retained in the LNs, but travel along the lymphatic tree towards venous circulation. These DCs can deliver their antigenic cargo to the spleen [48] and to primary lymphoid tissues (BM and thymus) [49, 50] (**Figure 3**). The migration of DCs, therefore, occurs in different environments, in different biophysical conditions and involves many cellular and molecular mechanisms.

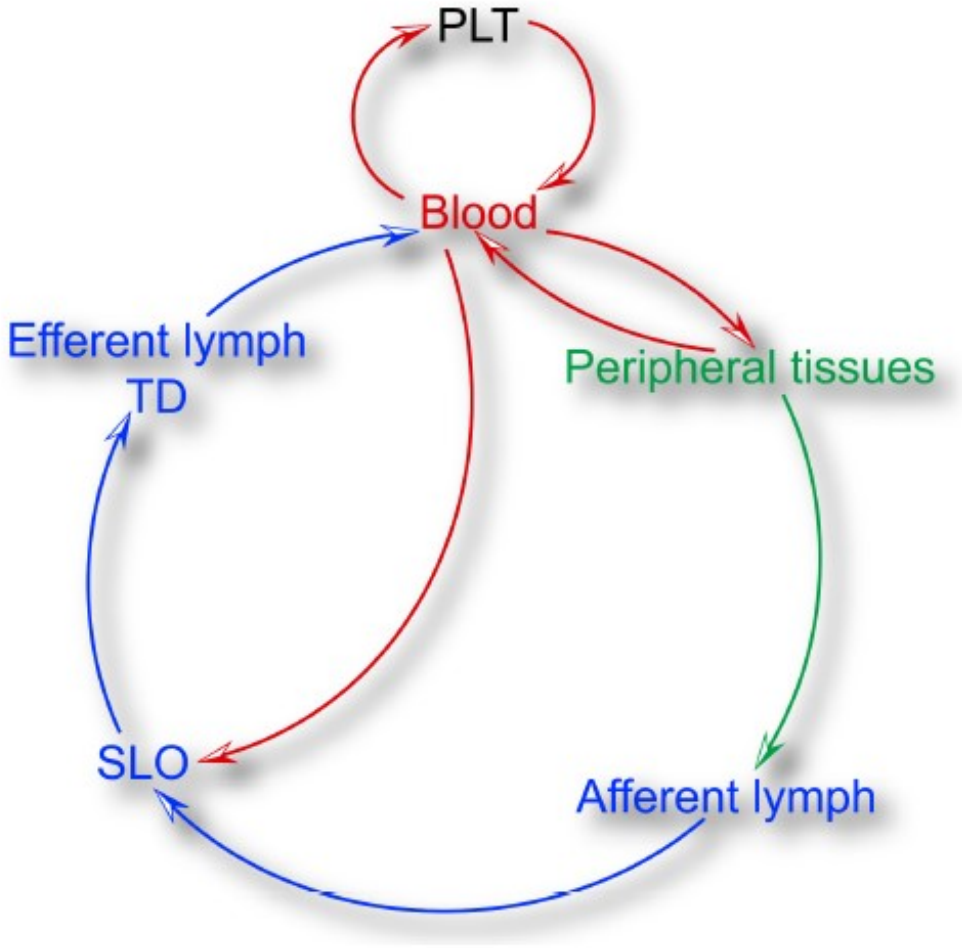

Figure 3. Dendritic cells migration ***(Alvarez, D. et al., 2008)***

2.3 Dendritic cells and Cancer-Immunity Cycle

DCs play a fundamental role in the antitumor immune response. These cells are necessary for T-cell-mediated cancer immunity. As inducers of a T cell response, they are critical for responses to cytotoxic and targeted agents [51].

Chen and Mellman summarized the interaction between cancer and immune system as a multi-step, multi-tissue, highly-regulated process, which they named the "Cancer-Immunity Cycle". Considering this definition, antitumor responses consist of a series of steps aimed at killing cancer cells. The generation of anticancer immunity is a cyclic process that can be self propagating, leading to an accumulation of immunostimulatory factors that should be amplify and broaden T cell responses (**Figure 4**) [27].

During the first step of the cycle, neoantigens created by oncogenesis are released and captured by DCs for processing (step 1). Subsequently (step 2), DCs present the captured antigens on MHCI and MHCII molecules to T cells, inducing in the priming and activation of effector T cell responses against the cancer-specific antigens (step 3). During these steps, the primary function of DCs is to sequentially acquire tumor antigen, migrate to the lymph node and activate a de novo T-cell response. However, only a small number of tumor DCs will migrate to the lymph nodes, probably this process is controlled by the expression of CCR7 [52]. Finally, the activated effector T cells transit to (step 4) and infiltrate the tumor (step 5), recognize and bind to cancer cells through the interaction between its TCR and its cognate antigen bound to MHCI (step 6), and kill their target cancer cell (step 7).

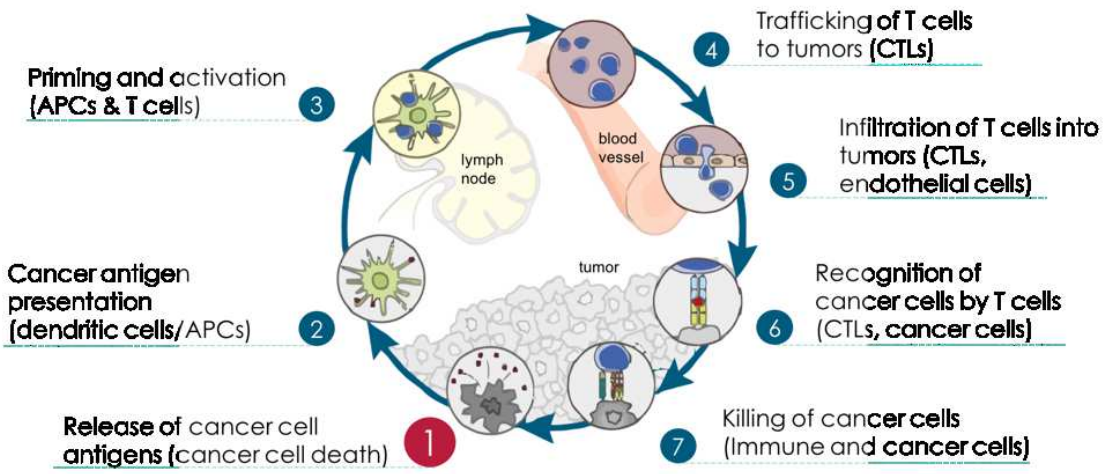

Figure 4. The Cancer-Immunity Cycle ***(Chen, D.S. et al., 2013)***

2.4 Hyperthermia and metabolic reprogramming of dendritic cells

Reprogramming energy metabolism has been described as an emerging hallmark in cancer cells [53].

Metabolic processes have been shown to have specific effects on the function of dendritic cells and that alteration, even if only one of these processes can modify the whole functioning of these cells [54, 55].

Recently, we have studied how exposure at 39°C for 3h in moDCs can induce alterations in the metabolic phenotype. Specifically, we have focused our attention on the activity of mitochondrial respiration and oxidative phosphorylation (OxPhos). Our results demonstrated the decrease in mitochondrial respiratory chain activity with a consequent decrease in oxidative phosphorylation, an increase in reactive nitrogen and oxygen species (RONS) production, and accumulation of intramitochondrial (mt) of Ca^{2+} ions ($mtCa^{2+}$). This process is accompanied by an increase in glycolysis, thus allowing us to hypothesize a metabolic rewiring and release of pro-inflammatory cytokines. Most likely, at the base of these phenomena there could be HSP70 and/or IGFBP6 [56, 57] (**Figure 5**).

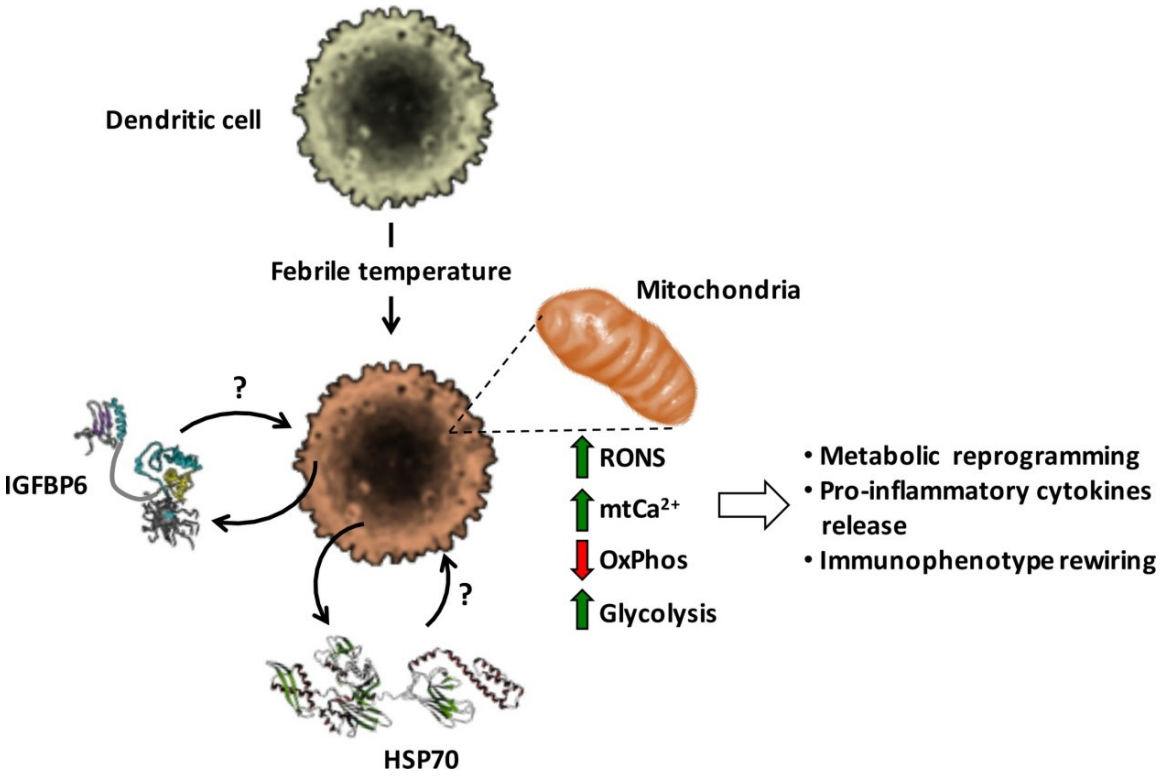

Figure 5. Effect of mild hyperthermic conditioning on MoDCs *(Liso, A. et al., 2018)*

3. Neutrophils, immunity and cancer

Neutrophilic granulocytes (neutrophils) are the most abundant leukocytes in blood. These cells play a primary role in the innate immunity [58]. In general, the neutrophils were associated with acute inflammation, but, a number of studies show that neutrophils are key effector cells also in the orchestration of adaptive immunity in the resolution of chronic inflammatory response. Neutrophils are integrated in the activation, regulation and effector mechanisms of the innate and adaptive immune systems [59-61]. They are considered the first line of defense during inflammation and infections [60].

Neutrophils are characterized by the ability to act as phagocytic cells, to produce reactive oxygen intermediates (ROI) with antimicrobical potential and to release enzymes from their granules [60, 62]. Neutrophils store numerous molecules in three types of granules: primary, secondary and tertiary. Primary or azurophilic granules are characterized by the accumulation of antimicrobial proteins and proteases (MPO and elastase); secondary or specific granules, which contain high levels of iron-binding protein lactoferrin, and tertiary or gelatinase granules, which contain matrix metalloproteinases [61]. Secondary and tertiary granules contain an overlapping set of proteins. More recently, a fourth granule has been described that was enriched in the microbial lectin ficolin-1 [63].

Neutrophils play an important role in inflammation within the tumor as they are attracted by CXCR2 ligands like CXCL1, CXCL2 and CXCL5, among others [64, 65]. High levels of neutrophils expression have been associated with detrimental outcome in several solid tumors [66]. The role of these cells in cancer is not fully understood, and as a hallmark of cancer, they reflect a state of host inflammation [53]. They can participate in different stages in the oncogenic process, including initiation, growth and proliferation, dissemination to the other tissues, and formation of new blood vessels in the tumor (**Figure 6**) [64, 67].

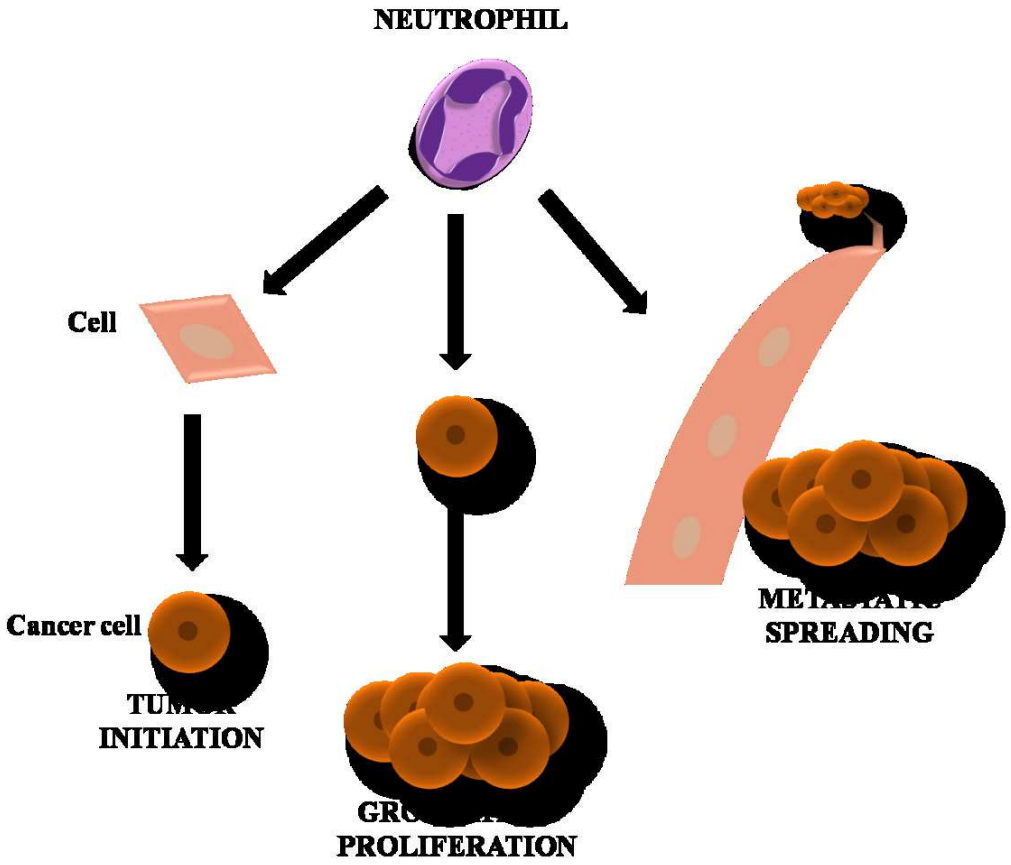

Figure 6. Neutrophils and oncogenic process

Early studies suggest that tumor-associated neutrophils (TANs) did not play a primary role in chronic and progressive diseases, such as cancer. However, more recently it is becoming clear that TANs have a significant function in tumor disease. In fact, neutrophils are considered potent antitumor effector cells [68]. These cells play an important role in antitumor activities thanks to the various antimicrobial and cytotoxic compounds contained in the granules that can destroy malignant cells; moreover, cytokines and chemokines secreted by neutrophils can also recruit other cells with antitumor activity [61, 69]. Neutrophils can facilitate tumor cells proliferation by attenuating the immune system. For example, neutrophils may suppress $CD8^+$ T lymphocyte antitumor response by releasing nitric oxide synthase (iNOS), or arginase 1 (ARG1) under TGF-β stimulation [70, 71].

Neutrophils can be activated by direct contact with T cells or DCs, as well as by locally produced cytokines, such as in the case of T_H17 cells, which have been shown to recruit these cells in CXCL-8-dependent manner [72].

4. Insulin-Like Growth Factor Binding Protein 6 (IGFBP6)

Insulin-like growth factor binding proteins (IGFBPs) are a group of secreted proteins involved in the transport of insulin-like growth factors (IGFs) with high affinity, regulating the bioavailability and function of IGFs. The IGFBP family consist of six proteins, IGFBP 1-6 [73, 74], however other proteins with low binding affinity to IGFs were incorrectly named as IGFBP7, IGFBP8, IGFBP9, etc. [75]. IGFBP 1-6 are composed of a three-domain structure [73]. The N-domain contains a highly conserved high affinity IGF binding subdomain that has two disulfide linkages that stabilize a globular structure containing a three stranded anti-parallel β-sheet [76]. IGFBP6 has structural and functional characteristics distinct compared to the other members of the IGFBPs family [77-79]. In IGFBPs 1-5, the N-terminal subdomanins contain a conserved GCGCC motif, with four disulphide bonds [80], whereas, IGFBP6 differs from the other IGFBPs as it is lacking this cysteine-rich motif and has only three disulfide bonds [81]. Moreover, this region of IGFBP6 has a different three-dimensional structure than that of the other IGFBPs [82]. The C-domains of IGFBPs 1-6 share sequence homology and are made up of three homologous disulphide bonds. Each domain consist of three homologous disulphide linkages, a conserved CWCV sequence and a thyroglobulin type 1 fold comprising an α-helix followed by a loop, a three-stranded antiparallel β-sheet incorporating a second loop and a disulphide-bonded flexible third loop [78, 83]. C-domain plays a key role in linking with IGFs. Many IGF-independent actions are mediated by the interaction of the C-domain with other proteins or glycosaminoglycans [73]. Due to the different structure, unlike the other IGFBPs 1-5, IGFBP6 binds IGF-II with an affinity greater than about 50 times the binding affinity with IGF-I [84]. IGFBP6 may undergo post-translational modifications, such as glycosylation, phosphorylation and proteolysis [85]. IGFs actions are mediated by binding to receptors, namely IGF type I receptor (IGF-IR), IGF type II receptor (IGF-IIR), insulin receptor type A (IR-A), insulin receptor type B (IR-B) and hybrid insulin/IGF-I receptor [86].

IGFBP6 is highly conserved across species, in fact, human *IGFBP6* shares 70–85 % sequence identity with rat, mouse, bovine and pig *IGFBP6* [87].

IGFBP6 protein is well known to inhibit the actions of IGF-II including proliferation, differentiation, migration and survival in many cell lines [77, 78], is a tumour suppressor and inhibits growth by an IGF-II-dependent mechanism (**Figure 7**).

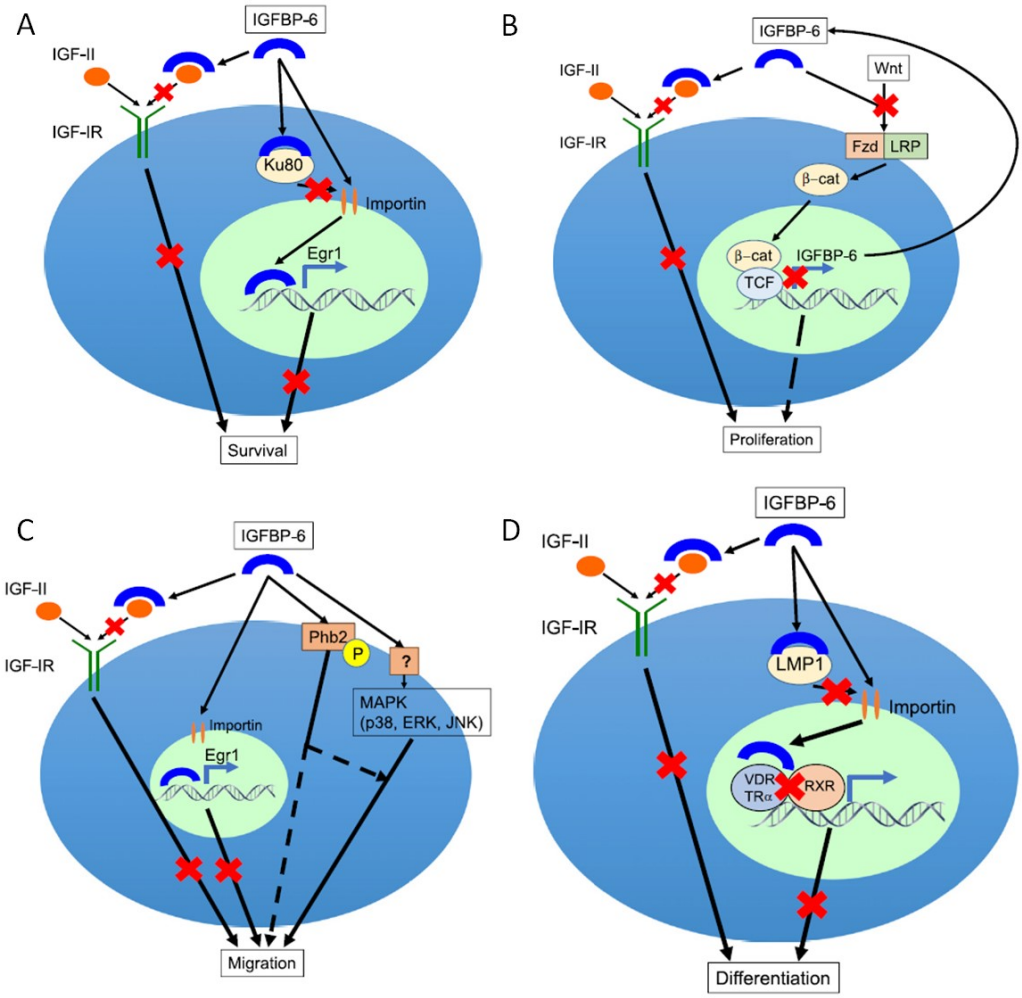

Figure 7. Effects of IGFBP6 on cell survival, proliferation, migration and differentiation (*Bach, A.L. 2016)*

Although the main IGFBP6 biological function is binding with IGF-II, it can also carry out functions independent of the IGF system [88]. IGFBP6 inhibits IGF-II actions but has little effect on IGF-I [78]. Numerous studies indicate that IGFBP6 inhibits angiogenesis and promotes cell migration by IGF-independent mechanisms, and enters the nucleus where it modulates differentiation and survival [86]. In contrast to other IGF binding proteins, IGFBP6 is a negative regulator of cellular senescence in the human fibroblasts; in fact, IGFBP6 over-expression increases the cellular lifespan [89]. However, recent studies suggest novel actions independent of IGF. In particular, IGFBP6 has been shown to induce chemotaxis in Rh30 rhabdomyosarcoma cells [90], to regulate cell apoptosis and migration in glioma [91], to be a novel nasopharyngeal carcinoma prognostic biomarker [92], to inhibit angiogenesis and to promote cell migration [86]. The migratory response mediated by IGFBP6 was due to the activation of MAP kinase pathway and possibly other signalling pathways [79].

4.1 Effect of IGFBP6 on cell survival

IGFBP6 can impair survival by inhibiting IGF-II actions but also by increasing EGR-1 transcription in an IGF-independent manner. This protein can exert intracellular actions through its translocation to the nucleus. In 2010, Iosef et al., showed that IGFBP6 specifically binds Ku80. Ku80 competes with importin-α in binding IGFBP6, using the same binding site (**Figure 7A)**.

Ku80 is a component of the Ku complex and it is required for proper telomere maintenance [93]. Intracellular IGFBP6 interacts preferentially with Ku80 during mitosis, thus regulating the availability of Ku proteins and indirectly influencing the DNA repair process [94].

4.2 Effect of IGFBP6 on cell proliferation

IGFBP6 can impair cell proliferation by inhibiting IGF-II actions but also by inhibiting Wnt/β-catenin signaling. Wnt/β-catenin pathway contains Wnt proteins, Frizzled (Fzd) receptor families, low-density lipoprotein-related protein receptors (LRP), cytoplasmic proteins, such as Dishevelled (Dsh), glycogensynthase kinase 3 (GSK3), APC, and transcription factors such as β-catenin (β-cat), Axin, T-cell factor/lymhoid enhancer factor (TCF/LEF) [95, 96]. Wnt signaling pathway is associated with oncogenesis in various cancers and play an important role in the

development of the central nervous system [97]. The translocation of β-catenin from the cytoplasm to the nucleus involves the binding of Wnt to its Fzd receptor and the LRP5/6 co-receptor. Only following the translocation, β-cat can modulate the transcription. *IGFBP6* is directly down-regulated by the β-cat/TCF complex in desmoid tumors. Desmoid tumors are aggressive fibromatosis in witch β-cat-mediated TCF-3-dependent transcription is activated. Starting from this evidence, IGFBP6 can be defined as target gene [98] (**Figure 7B**).

4.3 Effect of IGFBP6 on cell migration

IGFBP6 can enhance or inhibited cell migration by an IGF-dependent and/or independent mechanism. This protein enhance cancer cell migration by an IGF-independent manner that include binding to cell surface prohibitin-2 (Phb2) and/or MAP kinase pathway activation [86, 90]. Action of Phb can be modulated by phosphorylation and they also regulate intracellular signaling pathway, including MAP kinases [99]. MAP kinases (including JNK, p38 and and ERK) are implicated in cell migration and invasion [100]. In contrast, IGFBP6 can impair migration by an IGF-II-dependent action and by promoting EGR-1 transcription (**Figure 7C**).

4.4 Effect of IGFBP6 on cell differentiation

As shown in **Figure 7D**, IGFBP6 has been reported to inhibit the differentiation of myoblast and osteoblasts [101]. In particular, this protein can impair differentiation by inhibiting IGF-II actions but also by modulating cytoplasmic-nuclear translocation of LIM mineralization protein-1 (LMP-1) and nuclear receptor-mediated transcription by an IGF-independent mechanism [84]. LMP-1 is an intracellular osteogenesis regulator. This function is exerted through the up-regulation of bone morphogenetic proteins (BMPs) [102]. Overexpression of IGFBP6 alters the intracellular localization of LMP1 to the perinuclear region and suppresses the differentiation of human and murine osteoblasts. In addition, IGFBP6 and LMP-1 physically interact and this interaction is functionally relevant [103].

IGFBP6 can inhibit osteoblast differentiation by also binding the vitamin D receptor (VDR) in the nucleus and potentially inhibiting RXR/vitamin D receptor dimerization [104]. Furthermore, IGFBP6 binds the thyroid hormone receptor-α1 (TRα) in the nucleus and inhibits liothyronine-mediated osteoblast differentiation [101].

4.5 IGFBP6 and cancer

IGFBP6 has been indicated to be involved in the development and progression of numerous tumor types and can be used as prognostic biomarkers in various malignancies [74]. In numerous studies, IGFBP6 expression is lower in malignant than normal cells, suggesting that it has an inhibitory effect. IGFBP6 inhibits proliferation and tumor development in a number of IGF-II-dependent cancers, including neuroblastoma [105], colon [106], ovarian [107], prostate [108] and rhabdomyosarcoma [109]. Some studies have shown the opposite, which may represent a compensatory response to increased IGF-II activity or may reflect IGF-II-independent actions. A number of brief examples in different cancers follow.

4.5.1 IGFBP6 in Rhabdomyosarcoma

Rhabdomyosarcoma (RMS) is a primitive pediatric malignant soft tissue sarcoma of skeletal muscle phenotype that arises from a primitive mesenchymal cell. There are two principle RMS subtypes, embryonal (ERMS) and alveolar (ARMS). ERMS mainly affects children younger than 10 years of age [110], whereas ARMS is predominantly found in adolescents and young adults [111]. The etiology and risk factors remain largely unknown. Despite mutations in components of the IGF system have not been detected [112, 113], dysergulation of IGF signalling is important in RMS transformation and progression [114, 115]. Thus, IGF-II is an autocrine growth factor for RMS, playing an important role in the development and progression of the disease [78].

As reported in section 4, IGFBP6 inhibits the tumorigenic properties of IGF-II-action. This distinctive function of IGFBP6 compared to other IGFBPs, makes this protein a potential therapeutic candidate for IGF-II-dependent pediatric malignancies, such as RMS, where it may be possible to inhibit IGF-II in the tumor environment with minimal effect on normal growth induced by IGF-I. Moreover, IGFBP6 also promotes RMS cell migration in an IGF-independent manner; this mechanism involves MAPK pathway activation [116, 117].

4.5.2 IGFBP6 in Nasopharyngeal Carcinoma

Nasopharyngeal carcinoma (NPC) is a malignant tumor, endemic in some areas including southern China, Southeast Asia, North Africa and the Arctic, but it is rare in Europe and in the American continent [118-122]. It comes from epithelial cells that cover the surface and line the nasopharynx [123]. The symptoms include neck

masses, epistaxis, nasal obstruction and discharge, headaches and other non-specific indicators. Furthermore, considering the anatomical localization, it shows a high metastatic rate (lung, liver and bone) [124] and is diagnosticated when it is in an advanced stage [125]. A few studies have provided the effects of IGFs and IGFBPs on NPC. IGF-IR is overexpressed in malignant NPC [126] and one *in vitro* study has proposed IGFBP6 as a tumor suppressor [127]. Chen et al., have demonstrated that IGFBP6 is differentially expressed in NPC tissues and positive IGFBP6 expression is correlated with reduced locoregional relapse and distant metastasis risk. This study suggests that IGFBP6 may be an independent prognostic biomarker for NPC [92].

4.5.3 IGFBP6 in Glioblastoma

Glioblastoma (GBM) is the commonest and the most lethal form of brain tumor in adults. A subset of human gliomas expresses IGF1 and/or IGF2 [128] and, IGF2 is related to the aggressiveness of some GBMs [129]. Furthermore, the expression of IGF-1R is associated with shorter survival and poor response to the immunotherapeutic drug temozolomide (TMZ) [130]. A recent study showed that chemosensitive tumor cells are a source of IGFBP6, and the secretion of this protein serves to inhibit GBM progression [131]. Additionally, it has been demonstrated that higher plasma IGFBP6 levels are associated with a better prognosis for GBM patients [132, 133]. Finally, overexpression of IGFBP6 induced apoptosis and inhibited migration of glioma cells [91].

4.5.4 IGFBP6 in Breast Cancer

Breast cancer (BC) is the most prevalent type of cancer in the word, and considered to be the most invasive cancer in women. Numerous epidemiologic studies have examined the association between components of the IGF system and female breast cancer [134]. One of the most important clinical problems in the treatment of $HER2^+$ breast cancer is the development of tumor resistance. This resistance appears to be, in large part, due to IGF signaling [135]. In $HER2^+$ breast cancer model, the activity of the monoclonal antibody commonly used in therapy, such as trastuzumab (Herceptin) is interrupted by the increased expression of IGF-1R [136]. Furthermore, up-regulation of IGF-1R partially leads to a trastuzumab-resistance phenotype, while its down-regulation restores its sensitivity to the drug [137].

IGFBP6 expression is higher in breast cancer cells resistant to HER2 inhibition by trastuzumab than in sensitive cells, but its functional consequences are not studied

[138]. A few studies indicate that IGFBP6 can be defined as a new diagnostic marker in patients with breast cancer [139].

4.5.5 IGFBP6 in Ovarian Cancer

Ovarian cancer (OC) is the sixth commonest tumour in women [140] and is most lethal gynecologic cancer [141]. IGF-II has an important role in ovarian cancer; its levels predict poor survival in advanced stage [142]. IGFBP6 is expressed at low levels in ovarian cancers [143]. *In vitro* studies show opposite effects on the migration of HEY and SKOV3 ovarian cancer cells, but in both cases IGFBP6 activates the MAP kinase pathway [107]. These findings require further study.

4.6 IGFBP6 and autoimmune diseases

Recent studies have focused on the use of IGFBPs as biomarkers in autoimmune diseases, highlighting a diagnostic role. Moreover, several studies have shown the potential role in the diagnosis and monitoring of autoimmune diseases by IGFBP6 (and other IGFBPs). Nevertheless, the mechanism by which this function is explained remains partially unknown. A number of brief examples in different autoimmune diseases follow.

4.6.1 IGFBP6 as biomarker in Diabetes Mellitus

Type 1 diabetes mellitus (T1DM) is an organ-specific autoimmune disease characterized by progressive destruction of pancreatic β cells, resulting in insulin deficiency and hyperglycemia [144]. The pathogenesis of T1DM appears to be different when compared with type 2 diabetes mellitus (T2DM). However, recent studies show that there are autoimmune aspects also in T2DM. This theory is based on the presence of circulating autoantibodies against β cells, self-reactive T cells, but also on the glucose-lowering efficacy of some immunomodulatory therapies in T2DM [145]. Due to the close relationship to insulin, the IGF system and its binding proteins has been explored as a biomarkers in diabetes. In particular, the IGFBP6 serum levels modifications are correlated with diabetic retinopathy (RP) both in T1DM and in T2DM [146]. Furthermore, circulating levels of IGFBP6 may be useful in predicting the onset of complications in patients with T1DM. Numerous studies have shown a moderation increased of IGFBP6 in patients with T1DM and a severe increased in patients with diabetic complications such as nephropathy, photocoagulation, RP, blindness, foot ulcer, coronary artery disease (CAD),

hypertension (HTN), amputation, and peripheral neuropathy [147, 148]. These studies mainly addressed IGF-II-dependent effects of IGFBP6 and speculated that the increase of protein levels in T1DM patients can be the consequence of increased IGF-II levels induced by chronic hyperglycemia [147].

4.6.2 IGFBP6 as biomarker in Rheumatoid Arthritis

Rheumatoid arthritis (RA) is a systemic inflammatory disorder that predominantly affects the joints. The profile of IGFBPs were first characterized in the synovial fluid (SL) of RA patients, in which IGFBP2, IGFBP3 and IGFBP4 level were elevated compared to healthy donors (HD) or osteoarthritis patients (OA) [149-152]. More recently, Alunno et al., have demonstrated an increased IGFBP6 levels in RA synovial tissue (ST) compared to OA ST and a decreased of IGFBP6 levels in RA SL compared to OA SL. Furthermore, *in vitro* experiments showed that IGFBP6 acts as chemoattractant for RA immune cells (T cells) and this effect was partially inhibited by dexamethasone [153]. This study suggests a pathogenic role of IGFBP6 in RA and supports its therapeutic role.

5. Materials and Methods

5.1 Ethics Statement

Specific approval of the local ethics committee was obtained for this study (Ospedali Riuniti University Hospital cod. 30/CE/2014). Written informed consent was obtained from all participants.

5.2 Monocyte-derived Dendritic Cells Isolation

Nine consecutive healthy adult blood donors were recruited without regard to age, ethnic origin, or gender. Peripheral blood mononuclear cells were isolated from buffy coats by Lymphoprep^{R} densiy centrifugation resuspendend in AIM-V serum-free medium (Thermo FisherScientific) and seeded on T25 flasks. After overnight incubation at 37°C, nonadherent cells were removed and adherent cells were cultured for 6 days with 50 ng/mL GM-CSF and 1000 U/mL IL-4 for six days in a humified 5% CO_2 incubator at 37 °C [38].

In order to confirm DC phenotype, cells were stained with specific mAbs for 30 minutes at 4°C in FACS buffer Dulbecco's PBS (Lonza, Basel, Switzerland) containing 2% FBS (PAA GmbH, Pashing, Austria), washed twice and resuspended in cold FACS buffer with 0.1 μg/mL propiudium iodide (PI) (Carl Roth, Karlsruhe, Germany). Subsequently, stained cells were analyzed with Epics XL-MCL^{TM} flow cytometer (Beckman Coulter, Brea, CA, USA). Cell debrids and dead cells were excluded from analysis by gating on proper forward and sideward light scatter and on PI negative cells (~98%). For each condition, a minimum of $1x10^4$ living cells were analyzed. The results obtained were analyzed using Expo 32 ADC Software (Beckman-Coulter).

In order to confirm the DC phenotype, the following antibodies were used: anti-CD14; anti-CD80; anti-CD11c; anti-CD83; anti-HDRII (Beckman-Coulter). Some flasks were incubated at 39°C for 3 or 24 hours. For each experimental condition, appropriate controls were set up at 37°C.

5.3 Gene Expression Profiles: Sample Preparation and Hybridization

Cells were lysed in TRIZOL (Invitrogen, Frederick, MD, USA) and total RNA was purified with the QIAGEN RNeasy kit following manufacturer's instructions. RNA was quantified with the NanoDrop ND-1000, while, the quality was checked with the 2100 Bioanalyzer (Agilent Technologies, Santa Clara, CA, USA). Five μg total RNA

were transcribed from a T7-oligo (dT) primer with SuperScript II polymerase (Invitrogen). cDNA was then purified on affinity columns and in vitro transcribed with the T7 RNA polymerase and a biotinylated dUTP. Labeled cRNA was purified on affinity columns and quantified on the NanoDrop ND-1000. Twenty µg of cRNA were fragmented and the quality was verified with the Bioanalyzer 2100 (Agilent Technologies). The biotinylated cRNA was hybridized using the Affimetrix HGU133 Plus 2.0 array, containing about 55,000 probe sets and reading frames opened by the genome databases H. sapiens GenBank, dbEST and RefSeq. The chips were scanned into the Affimetrix Complete GeneChip® Instrument System, resulting in digitized image data (DAT) files.

5.4 Microarray Data Analysis

DAT files were analyzed by Expression Console (Affymetrix Inc.). In order to normalize the full data set, the Robust Multi alignment Algorithm [154] was used. The expression values were analyzed by using GeneSpring GX 10 (Agilent Technologies). Further normalization steps included per-chip normalization to 50th percentile and per-gene normalization to median. Normalized data were filtered for fold changes greater than 2, giving a list of 67 genes on 83 probe sets. This set of differentially expressed genes constitutes our "focus gene list". The fold change represents the ratio between the averages of the normalized expression values at temperatures of 39°C and at 37°C. Microarray data are available in the ArrayExpress database (www.ebi.ac.uk/arrayexpress) with the following access number E-MTAB-697.

5.5 Analysis of Gene Expression Data

The analysis algorithm from Ingenuity Pathway Analysis (IPA; Ingenuity® Systems, www.ingenuity.com) was used in order to identify the biological functions (IPA's biofunction tool) and knowledge-based networks (IPA's network generation tool) from the differentially expressed focus genes. By exploiting the biological information stored in the Ingenuity Pathway Knowledge Base (IPKB) it was possible to highlight the biological functions and/or diseases associated to the considered data sets. Focus genes were associated with biological functions and/or diseases in the IPKB.

In order to calculate the probability (p-value) that each biological function/disease association is due to chance alone, the exact Fisher test was used [155]. Finally,

resulting p-values were corrected for multiple tests using the Benjamini-Hockberg False Discovery Rate (FDR) [156].

5.6 Cell Lines

Numerous cell lines have been used, among them: Human Renal Tubular (HK2), Human Aortic Endothelial Cells (HAEC), Human Colon Cancer (HCT116), Human Breast Adenocarcinoma (MCF-7 Cells), Human Prostate Cancer (PC3) and heterogeneous Human Epithelial Colorectal adenocarcinoma (CACO2).

HK2 cells were cultured in 50% DMEM and 50% HAM's F12 supplemented with 10% fetal bovine serum, 2 mM L-glutamine, 100 IU/ml penicillin and 100 µg/ml streptomycin (Invitrogen).

HAEC were cultured in EBM™-2 (endothelial basal Medium-2), supplemented with EGM™-2 BulletKit™ (EBM™-2 plus SingleQuots™ of growth supplements) containing BBE (Bovine Brain Extract), hEGF, hydrocortisone, GA- 1000 (Gentamicin, Amphotericin-B), FBS (Fetal Bovine Serum), VEGF, hFGF-B, R3-IGF-1, ascorbic acid, heparin (Lonza).

HCT116, MCF-7 Cells, PC3 and CACO2 were cultured in Dulbecco's modified Eagle's medium (DMEM) supplemented with 10% fetal bovine serum (FBS), 1% PenStrep (10,000 U/mL Pen, 10 mg/mL Strep) 2 mM L-glutamine (medium and reagents from Sigma- Aldrich, Milan, Italy).

5.7 Real Time RT-PCR Analysis

For each sample, we isolated the total RNA using TRIZOL (Invitrogen), quantified the RNA using the NanoDrop-ND-1000 and checked the quality with the 2100 Bioanalyzer using the average A260/280 ratio of 2.0. Three µg total RNA were used in a from a 20 µl reaction mixture using Oligo (dT) primers and cDNA SuperScript II (Invitrogen). For real-time PCR, the following primers were used: IGFBP6, forward 5'-GGAAGCTGAGGGCTGTCTC-3', reverse 5'-GTCTCTGCGGTTCACATCCT-3'; ARMET forward 5'-CTGAGCACAGTGGACCT-3', reverse 5'-GGCTGTTTTGGGAGTAA-3'; PLAT forward 5'-AGGGCTGGAGAGAAAAC-3', reverse 5'-CTGGCTCCTCTTCTGAAT-3'; GAPDH forward 5'-CAAGGCTGAGAACGGGAA-3', reverse 5'-GCATCGCCCCACTTGATTTT-3'. Primers were designed to be intron spanning.

The size of the products was also confirmed by gel electrophoresis. mRNA levels were expressed relative to the housekeeping gene by comparing PCR threshold cycle

(CT) between cDNA of samples and GAPDH (ΔCT). Subsequently, relative gene expression was calculated as follows: fold change = 2-*Δ(ΔCT)*, where *ΔCT = CTtarget - CThousekeeping* and *Δ(ΔCT) = ΔCTtreated - ΔCTcontrol*. All experiments were performed in triplicate for each experimental condition. In order to assess the expression in both normothermia and hyperthermia for the three selected genes, the Student's t-test for paired data was used. All tests were two-sided and significance was set at $p<0.05$.

5.8 Flow Cytometry: IGFBP6 Production

After incubation for 3, 8, 24 and 48 h at 39°C moDCs were fixed in 3% paraformaldehyde and 2% sucrose in PBS and permeabilized (or not) with ice-cold Triton HEPES buffer (20 mM HEPES, 300 mM sucrose, 50 mM NaCl, 3 mM MgCl2, 0.5% Triton X-100, pH 7.4) for 5 min at room temperature. For each condition the respective control was analyzed after incubation at 37°C. Subsequently, cells were incubated with rabbit anti-human IGFBP-6 (Abcam; ab135606) for 1 h at 4°C (dilution 1:25), washed twice with PBS, and incubated with secondary antibody donkey anti-rabbit IgG (Alexafluor 488) for 30 minutes at 4°C (dilution 1:1000). Negative controls were set up by incubating the cells either only with secondary antibody or rabbit IgG, polyclonal - isotype control (Abcam, ab37415) followed by incubation with secondary antibody.

After fixation (or not), the number of dead cells was assessed using Zombie Aqua Fixable Viability kit (BioLegend, San Diego, USA). The labeled cells were washed twice with PBS and resuspended in 50µl of PBS 1X according to manufacturer's protocol. The cells were analyzed by AmnisFlowsight IS100 (Merck Millipore). By plotting the Area (a parameter related to the cellular dimension) on x-axis vs Aspect Ratio (a parameter reflecting the ratio of the cell Minor Axis divided by the Major Axis) on y-axis, scatter plots of the brightfield were obtained, and then single cells events were gated. Finally, 20,000 single-cell events for sample were acquired.

Using the Amnis IDEAS software the percentage of positive green cells (Channel 2, excitation laser 488 nm) and mean fluorescence were analyzed. The value of the negative control was subtracted from the values obtained. Brightfield and green fluorescent images for any single cell event were collected. A representative image of a single cell for any condition is shown (Paragraph 6.4; Figure 14). The data

obtained by Zombie Dye staining revealed that an average of 4% of unfixed cells and 10% of fixed cells were dead.

5.9 Analysis of IGFBP6 in Conditioned Medium

After 3, 8, 24 and 48 h exposure of moDCs to 39°C (or maintained at 37°C as control), conditioned media were harvested and centrifuged at 200 x g at 4°C for 12 min and proteinase inhibitor (Aprotinin, Boehringer Mannheim GmbH) was added. Secreted protein was detected using a Bio-Plex cytokine, chemokine and growth factor assay (Bioclarma, Turin, Italy).

According to manufacturer's instructions, the assay was performed in 96-well microplates using the Human IGF Binding Protein (IGFBP-6) Magnetic Beads Panel (HIGFBMAG-53K, Millipore) at the Bioclarma - Research and Molecular Diagnostics, Turin, Italy. Undiluted supernatant samples were drawn up into the Bio-Plex 100 System array reader (Bio-Rad). This reader identifies and quantifies each specific reaction based on the bead color and on the fluorescent signal intensity.

Data processing was done using the Bio-Plex Manager software (version 6.1) using the five-parametric curve fitting and converted to ng/mL. The concentration of IGFBP6 was obtained by comparing the fluorescence with that obtained from a standard curve (sensitivity limit of the assay: 0.04 ng/mL).

5.10 Apoptosis and Necrosis

In order to evaluate the rate of apoptosis/necrosis, after incubation for 3, 8, 24 and 48 h at 39°C (or 37°C as control), we used the FlowCellectTM Annexin Red Kit (Merck Millipore), according to the manufacturer's instructions. Then, the cells were stained with Annexin V conjugated with a sensitive CF647 dye (excitation laser: 642 nm, emission max: 670 nm) for 15 minutes at 37°C, washed in assay buffer and stained with 7-AAD (excitation laser: 488 nm, emission max: 642 nm) for 5 min and analyzed by AmnisFlowsight IS100 (Merck Millipore).

Brightfield aspect ratio versus brightfield area plots were generated to identify single cells events. For each condition, 20,000 single-cell events were acquired.

By plotting the fluorescence of AnnexinV (Channel 11) vs. fluorescence of 7-AAD (Channel 5), dot plots were obtained.

In dot plots it is possible to identify four different populations:

(1) healthy cells, Annexin $V^{(-)}$ and 7-$AAD^{(-)}$;

(2) necrotic cells, Annexin $V^{(+)}$ and 7-$AAD^{(+)}$;

(3) early apoptotic cells, Annexin $V^{(+)}$ and 7-$AAD^{(-)}$;
(4) late apoptotic cells, Annexin $V^{(-)}$ and 7-$AAD^{(+)}$.

5.11 Cell Chemotaxis

PBMCs were isolated from buffy coats of healthy donors and used to purify $CD14^+$ monocytes, $CD19^+$ B cells and $CD3^+$ T cells with magnetic microbeads kit (Miltenyi Biotec). We evaluated the chemotactic activity of IGFBP6 by adding monocytes, T and B lymphocytes (10^6 per filter) to the upper compartment of 0.33 cm^2 Transwells with 3 μm-pore filters (Corning, Acton, MA, USA), while no IGFBP6 (as a negative control) or different concentrations of IGFBP6 (Peprotech, London, UK) (0.01 μg/ml, 0.1 μg/ml, 1 μg/ml) corresponding respectively to 0.4, 4 and 40 nM were dissolved in serum free Eagle's Medium minimal essential medium (MEM, Sigma-Aldrich, Milan, Italy) in the lower compartment.

As a positive control, different concentrations of SDF-1 were used (Peprotech, London, UK). The concentrations added to the lower compartment are as follows: 0.05 μg/ml, 0.5 μg/ml, 1 μg/ml and correspond to 6 nM, 60 nM and 125 nM respectively. The SDF-1 concentrations used have been shown to be optimal for chemotaxis of monocyte, T and B lymphocytes [86, 90, 116].

To evaluate the specificity of the IGFBP6 chemotactic effect, before adding the mixture in the lower compartment, we pre-incubated the protein at the highest dose with a rabbit IgG anti-human C-terminal IGFBP6 antibody (Abcam, Cambridge, UK) or with an irrelevant rabbit IgG antibody (anti-human HVCN1, Abcam, Cambridge, UK) in a weight ratio (IGFBP6/antibody) of 1:6 for 30 minutes at room temperature. As a negative control, we used recombinant human/murine/rat (insect-derived) Activin A (Peprotech, London, UK), in the lower compartment at a dose of 40 nM.

Subsequently, after 150 min, cells were recovered in the lower compartment and quantified by flow cytometry. The data obtained were expressed as a percentage of migration of the control (100%).

5.12 Neutrophils Isolation

Five-seven consecutive healthy blood donors were recruited without regard to age, ethnic origin, or gender. Leukocytes were isolated by sedimentation on a Lymphoprep gradient. After blood stratification, peripheral blood mononuclear cells were eliminated and neutrophils and red blood cells were centrifuged. Pellet was

resuspended in 1800 μL hydrogen peroxide and after 10 seconds, the reaction was blocked in 200 μL PBS 10X.

5.13 Neutrophils: IGFBP6 and ROS Production

To investigate ROS production, neutrophils were treated with IGFBP6. We have added or not IGFBP6 (as a negative control) at different concentrations of IGFBP6 (Peprotech, London, UK) (0.01 μg/ml, 1 μg/ml, 5 μg/ml) corresponding respectively to 4, 40 and 200 nM were dissolved in serum free Eagle's Medium minimal essential medium (MEM, Sigma-Aldrich, Milan, Italy) for 50 minutes. In order to evaluate whether IGFBP6 may increase or potentiate other stimuli, cells were first incubated with IGFBP6 1 μg/ml for 50 minutes and then with either *N*-formyl-methionyl-leucyl-phenylalanine (fMLP) 1 μM or phorbol 12-myristate 13-acetate (PMA) 10 nM for 5 minutes. As a positive control, we used fMLP or PMA without the addition of IGFBP6. The fMLP and PMA concentrations used have been shown to be optimal for ROS production in neutrophils [157, 158].

After cells incubation with IGFBP6, with or without fMLP or PMA, cells were supplemented with 2,7-dichlorofluorescein diacetate (which is converted to dichluorofluorescein-DCF by intracellular esterases) for 10 minutes, washed with PBS, resuspendend in 50 μl PBS and then analyzed by AmnisFlowsight IS100 (Merck Millipore).

5.14 Degranulation in Neutrophils

In order to test the involvement of IGFBP6 in degranulation of primary and tertiary granules, neutrophils were pre-incubated with IGFBP6 1 μg/ml for 50 minutes and then with either fMLP 1μM or with IGFBP6 alone. Then, culture supernatants were collected and stored at -80°C until enzymes quantification. Degranulation was studied in terms of release of myeloperoxidase (MPO; primary granules), matrix metalloproteinase (MMP-9) and TNF-α by ELISA (R&D Systems, Minneapolis, MN, USA).

5.15 Transwell Migration Assay

Human neutrophils were isolated by Lymphoprep's blood stratification ad described in section 5.12 and then were suspended in PBS 1X.

The transmigration through the epithelium was evaluated in the basolateral to apical direction ('down' mode) in monolayers grown 3-μm-pore filters. 7 ×

10^4 cells were plated on the bottom Transwells (Corning, Acton, MA, USA) for 48 h and then the filters were inverted [159, 160]. Medium was added both in the lower and upper compartments. After 7 days from seeding of epithelial cells, neutrophils were added in the upper compartment (10^6 per filter), i.e., from the basolateral side, while in the lower compartment, ie, from the apical side, different concentrations of IGFBP6 (Peprotech, London, UK) was added. The concentrations of IGFBP6 used are shown below: 0.01 μg/ml, 1 μg/ml, 5 μg/ml, corresponding respectively to 4, 40 and 200 nM. After 150 minutes, cells were recovered in the lower compartment and quantified by flow cytometry. In order to evaluate whether IGFBP6 could have a priming effect, neutrophils were pre-incubated with IGFBP6 1 μg/ml for 50 minutes, and were then added to the basolateral side of the epithelium in the presence of apical fMLP 1 μM. As a positive control, fMLP was used [159]. The data obtained were expressed as a percentage of migration of the control (100%).

5.16 Statistical analysis

Data obtained from apoptosis/necrosis and chemotaxis experiments in moDCs are shown as mean ± standard error of the mean (SEM) and analyzed for statistical significance using 2-way ANOVA with Tukey's Multiple Comparison test using Graphpad Software v. 4 (La Jolla, CA, USA). $P<0.05$ was considered statistically significant.

Neutrophils data presented shown mean ± SEM and analyzed using two-tailed Student's *t* test using Software v. 4 (La Jolla, CA, USA). *P* values <0.05 were considered to be statistically significant.

6. Results

6.1 moDCs exposed to mild hyperthermia present a distinct gene expression profile

Gene expression profile was performed on nine healthy donors. In all cases, moDCs were obtained from buffy coats. After monocytes isolation, cells were differentiated into monocyte derived-dendritic cells (moDCs). In order to evaluate the phenotype in normothermia or hyperthermia, cells were incubated at 39°C for 3 and 24 h (or 37°C as a control) **(Figure 8)**. Data shown that **incubation at 39°C for 3 and 24 h** resulted in a significant **increase** of percentage of cells expressing **maturation markers** (such as CD11c, CD80, CD83, and HDRII), but not of CD14, if compared to the control at 37°C.

Gene expression analysis demonstrated that the exposure of moDCs for 3 h at 39°C causes a significant **increase** in the **expression of 43 genes** and a **decrease of** another **24 genes** if compared to the expression of normothermic cells **(Table 1)**. A biologically meaningful effect was defined as significant when a greater than 2-fold difference was detected in all experiments.

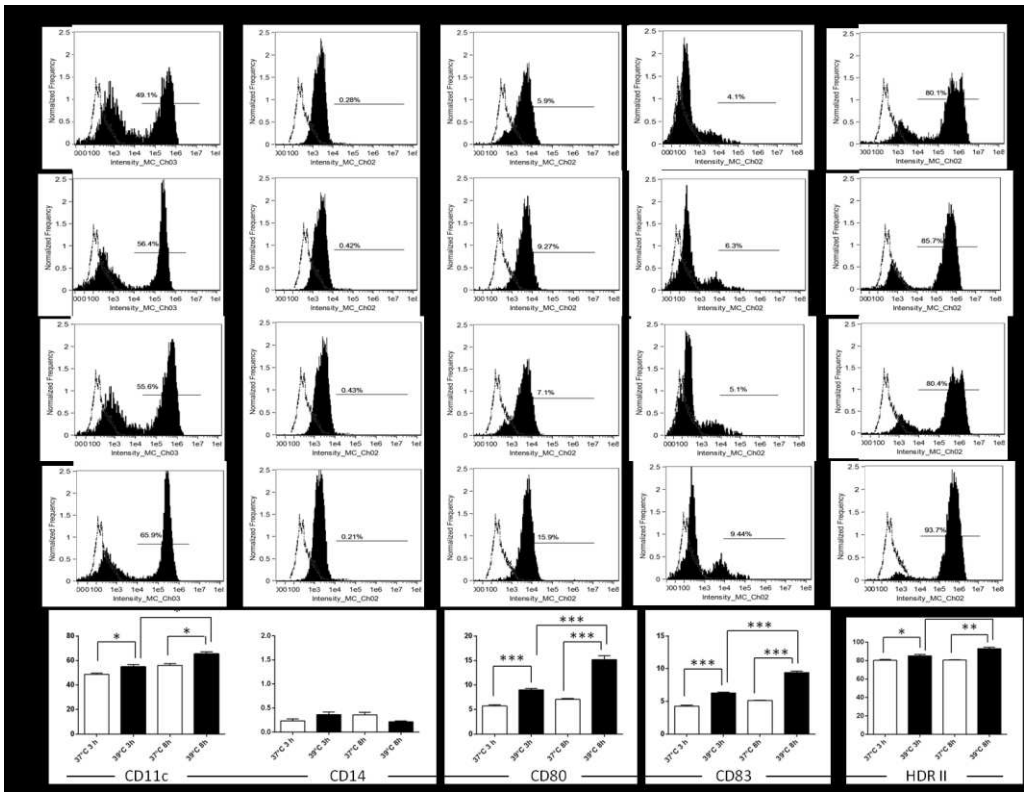

Figure 8. Phenotypic characterization of moDCs. Phenotypic characterization of monocyte-derived dendritic cells was performed after differentiation and incubation for 3 h at 37°C (**A**) and 39°C (**B**) and for 24 h at 37°C (**C**) and 39°C (**D**) by staining them with specific antibodies (black filled histograms). Unstained controls are shown as dotted lines. The panels are representative of one case of the nine analyzed for gene expression. **E.** The percentage of maturation markers after exposure at 39°C and 37°C at different times. Data are representative of four separate experiments. All data represent means ± SEM of four independent experiments. Statistical comparisons were made using the unpaired Student's t-test. *p<0.05; **p<0.001; ***p<0.0001.

Downregulated		
	Gene Symbol	Fold change
228603 at	ACTR3	2.1212146
226025 at	ANKRD28	2.3790717
233011 at	ANXA1	2.3608308
225166 at	ARHGAP18	2.2429798
235088 at	C4orf46	2.0362923
229695 at	fam107b	2.348431
1554678 s at	HNRPDL	2.129529
204334 at	KLF7	2.6032488
230636 s at	KLF9	2.1131873
240655 at	LOC100133690	2.1164844
244846 at	MAP4K4	2.2667267
1558111 at	MBNL1	2.2078938
1569030 s at	NUB1	2.0441904
214963 at	NUP160	2.017219
225626 at	PAG1	2.0477161
213933 at	PTGER3	2.5118344
554999 at	RASGEF1B	3.3729293
226312 at	RICTOR	2.2310023
209684 at	RIN2	2.0676558
220123 at	SLC35F5	2.102914
215078 at	SOD2	2.2981791
226837 at	SPRED1	2.4078321
207983 s at	STAG2	2.0910532
217833 at	SYNCRIP	2.120536

Upregulated					
	Gene Symbol	Fold change		Gene Symbol	Fold change
201491 at	AHSA1	3.0668783	201841 s at	HSPB1	2.105686
217911 s at	BAG3	3.3147337	200806 s at	HSPD1	3.5899048
219966 x at	BANP	3.369214	200807 s at	HSPD1	2.923671
228928 x at	BANP	2.9106443	205133 s at	HSPE1	3.3237238
233186 s at	BANP	2.674547	235573 at	HSPH1	3.050632
211761 s at	CACYBP	2.099444	208744 x at	HSPH1	6.470141
210691 s at	CACYBP	2.2031457	206976 s at	HSPH1	8.415396
206331 at	CALCRL	2.0365825	200825 s at	HYOU1	2.0537353
210815 s at	CALCRL	2.2632575	210029 at	IDO1	2.4012868
200910 at	CCT3	2.1207094	203851 at	**IGFBP6***	2.2617126
218566 s at	CHORDC1	4.3639574	207901 at	IL12B	2.0140626
204170 s at	CKS2	2.359756	227140 at	INHBA	2.0002825
225434 at	DEDD2	2.2326558	202220 at	KIAA0907	3.196178
225061 at	DNAJA4	5.536901	1558404 at	LOC644242	2.2391515
1554334 a at	DNAJA4	4.3517003	218559 s at	MAFB	2.2515247
1554333 at	DNAJA4	2.3606193	202655 at	**MANF***	2.083146
200664 s at	DNAJB1	2.4289098	217907 at	MRPL18	2.3864717
200666 s at	DNAJB1	2.4802563	209785 s at	PLA2G4C	2.0645976
209015 s at	DNAJB6	3.323787	201860 s at	**PLAT***	2.0551631
213145 at	FBXL14	3.1741052	204186 s at	PPID	2.0264704
200894 s at	FKBP4	2.268422	212706 at	RASA4	2.0581238
200895 s at	FKBP4	2.213333	203164 at	SLC33A1	2.208336
222033 s at	FLT1	2.0301073	212009 s at	STIP1	2.211557
201503 at	G3BP1	2.117231	213330 s at	STIP1	3.3498967
214359 s at	HSP90AB1	2.6591988	223330 s at	SUGT1	2.3122559
200064 at	HSP90AB1	2.6207926	235542 at	TET3	2.130128
1557910 at	HSP90AB1	3.1781142			
200799 at	HSPA1A	2.4917276			
200800 s at	HSPA1A ///	4.0723443			
202581 at	HSPA1A ///	10.3153925			
230031 at	HSPA5	2.2923908			
211936 at	HSPA5	2.530812			
210338 s at	HSPA8	2.1047974			

* Genes also tested by RT-PCR are shown in bold

Table 1. Gene expression profile.

We found that exposure for 3h at 39°C causes up/down regulation of genes encoding proteins involved in post-translational modification (e.g., *NUB1* and *CACYBP*), cellular movement (e.g., *IDO1*), protein folding (e.g., *CCT3*), and cell death and survival (e.g., *ANXA1* and *KLF7*) **(Figure 9)**.

Our study allowed to further investigate the key role played by DCs in the response to heat shock.

As a control, we considered the upregulation of genes encoding heat shock proteins (*HSP90AB1, HSPA1A, HSPA1B, HSPA5, HSPA8, HSPB1, HSPD1, HSPE1, HSPH1*). These data indicate that **3 h-exposure to 39°C** may **increase the maturation of moDCs** and causes a **modification in the global gene expression profile of DCs**.

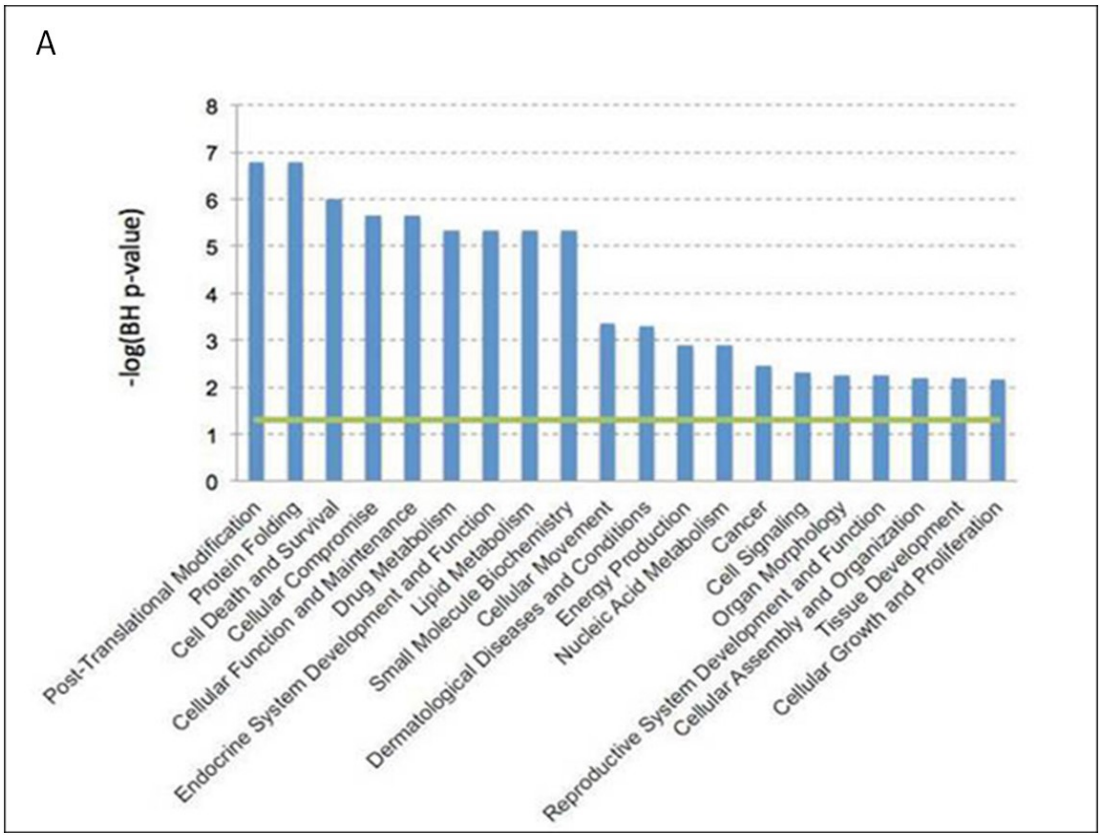

Figure 9. Gene expression profile data analysis. DCs expression profiles were evaluated by Affimetrix HUG133 Plus 2.0 array. Data were analyzed by Expression Console (Affimetrix Inc.). All the biological functions values exceeding the threshold (-log(BH) *p*-value)= 1.3), represented the green line, identified by the IPA-Biofunction tool are statistically significant.

6.2 moDCs and regulation of IGFBP6

The gene expression profile showed that some up-regulated **genes encode for secreted protein**, namely, ***MANF***, ***PLAT***, and ***IGFBP6***; we have focused our attention on these proteins because if a protein is secreted, it is a protein potentially capable of interacting with other immune cells through receptors.

Mesencephalic **A**strocyte-derived **N**eurotrophic **F**actor (*MANF*) also known as **A**rginine-**R**ich **M**utated in **E**arly **T**umors (*ARMET*) encodes for a secreted protein [161] localized in the luminal endoplasmic reticulum (ER). Apostolou et al., have shown that the reduced expression of MANF is linked to increased susceptibility to ER stress-induced death and cell proliferation [162]. Moreover, recent studies in rodent models have showed that this gene exerts neurotrophic function in neurodegenerative disease, mitigates diabetes, protect cardiomyocytes and neurons in

myocardial infarction and cerebral ischemia [163].

Tissue-type **P**lasminogen **A**ctivator (*PLAT*) is a gene that encodes a secreted serine protease (also known as tPA), which converts the proenzyme plasminogen to plasmin [164]. This enzyme plays a key role in cell migration, tissue remodeling and thrombus dissolution. Furthermore, plasma levels of tPA have been associated with cardiovascular disease [165].

Insulin-like **G**rowth **F**actor **B**inding **P**rotein **6** (*IGFBP6*) encodes for a secreted protein that inhibits tumorigenic properties of IGF-II dependent cancers [86]. IGFBP6 has been shown to induce chemotaxis in Rh30 rhabdomyosarcoma cells [90, 116], to regulate cell apoptosis and migration in glioma [91] and to be a novel carcinoma prognostic biomarker [92]. In order to confirm the up-regulation of *MANF*, *PLAT*, and *IGFBP6* in moDCs, RT-PCR was used. qPCR was performed on four healthy donors unrelated to the previous cohort. The data obtained allowed us to find that although there is an **up-regulation of the three genes** (**Figure 10A**), the **only gene** in which **statistical significance** could be demonstrated was ***IGFBP6*** (p=0.004), while, the PLAT up-regulation was not statistically significant (p=0.089). Probably, in the case of *MANF*, significance has not been reached due to the variability in expression levels in a small cohort. **These data show that exposure for 3 h at 39°C in moDCs causes a selective up-regulation of *IGFBP6*, suggesting *IGFBP6* as an early marker of fever-like temperature.**

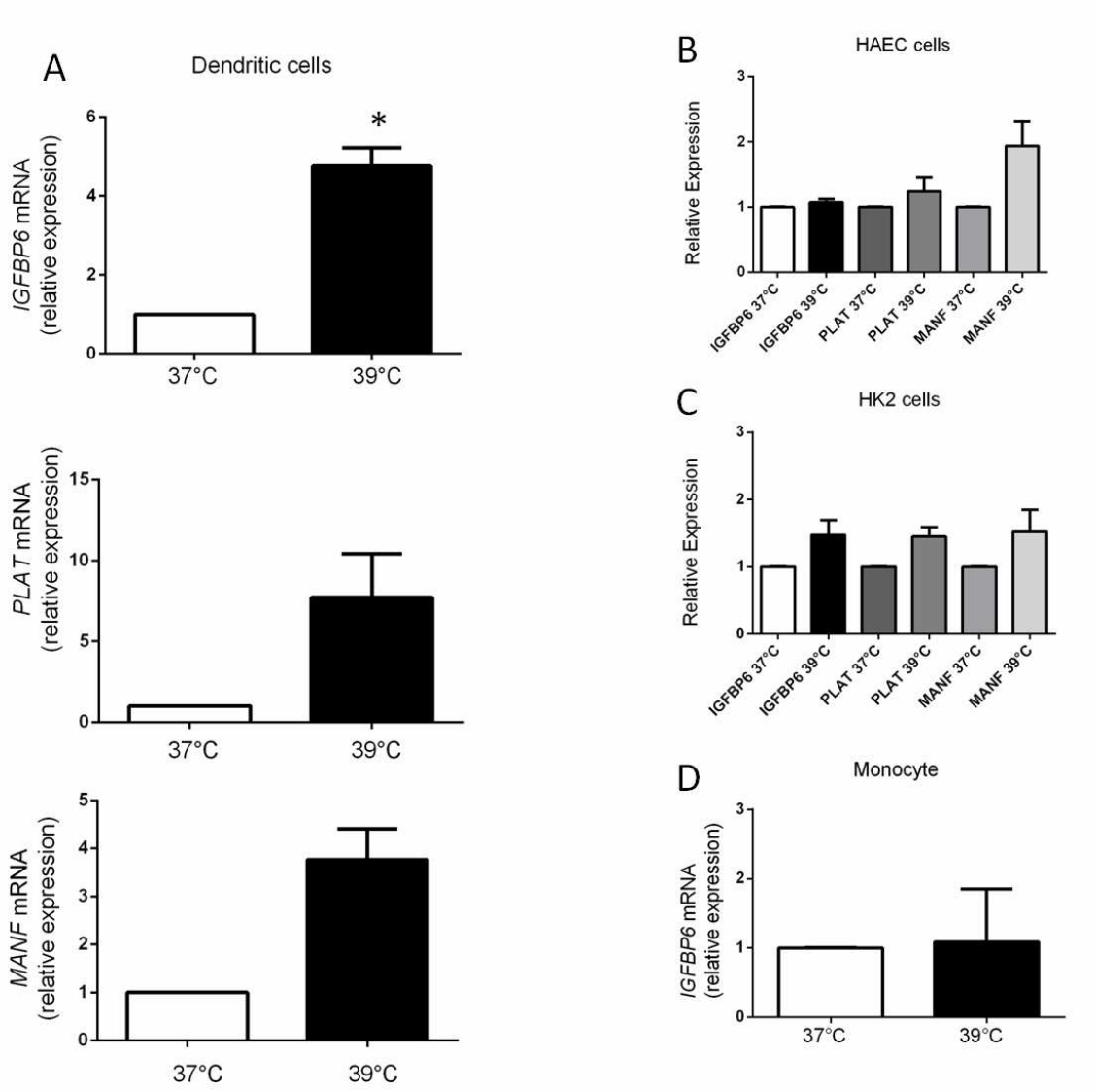

Figure 10. mRNA expression levels of *MANF, PLAT* and *IGFBP6* by RT-PCR. *MANF, PLAT* and *IGFBP6* mRNA expression in moDCs (**A**), HAEC (**B**), HK2 (**C**) and monocytes (**D**) for 3h at 39°C under control (37°C). **A**. Bars represent the mean ± SEM of four different triplicate samples. Statistical comparisons were made using paired data Student's test. Difference were considered significant when $p < 0.05$. **B., C., D.** Bars represent the mean ± SEM of three different triplicate samples. Statistical comparisons were made using paired data Student's test. Difference were considered significant when $p < 0.05$.

6.3 The up-regulation of *IGFBP6* is specific to moDCs

Subsequently, we investigated whether the up-regulation of *MANF*, *PLAT*, and *IGFBP6* is a general biological phenomenon and therefore present in various cell types or if any of those genes would be differentially regulated in moDCs compared to other cells exposed at 39°C. Thus, we compared expression as measured by qPCR in ontogentically distant cell lines and we found that, while in moDCs exposure for 3h at 39°C induces ~5-fold increase of *IGFBP6* expression, in human aortic endothelial cells (HAEC), in human kidney cells (HK2) and in a number of human tumor cell lines there is no gene up-regulation (**Figure 10B** and **10C**, **Figure 11**) *[166, 167]*. We also studied the expressions of *PLAT* and *MANF* in the two ontogenetically distant cell lines (HAEC and HK2). The expressions of both genes were not significantly up-regulated (**Figure 10B** and **10C**). In HAEC cells *p*-values for *IGFBP6, MANF* and *PLAT* were 0.26, 0.11, and 0.4 and in HK2 cells 0.16, 0.25, and 0.7 respectively.

In order to understand if the up-regulation was a characteristic phenomenon of the dendritic line, we evaluated if monocyte *per se* up-regulated *IGFBP6* expression after exposure to hyperthermia. Surprisingly, we found that in this cell line *IGFBP6* is not up-regulated (p=0.9) (**Figure 10D**).

These data indicate that **up-regulation of IGFBP6** by hyperthermia **is a specific in moDCs** and therefore **could play a specific role in the physiology of DCs**. Considering the consistency of the data obtained, and in order to clarify its biological role in DCs, we decided to focus our attention only on *IGFBP6*.

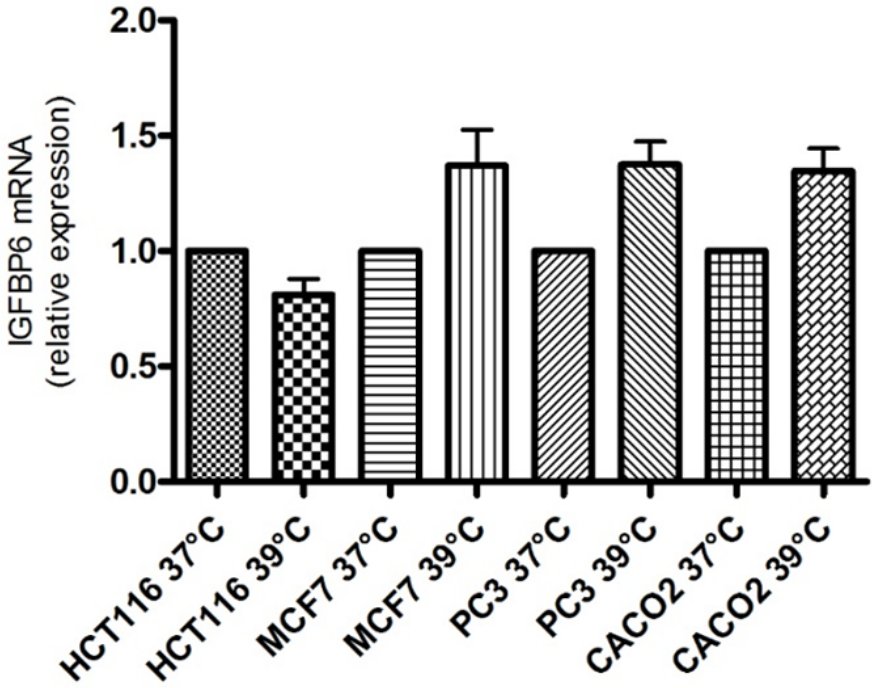

Figure 11. Expression levels of *IGFBP6* by RT-PCR in ontogenetically distant cell lines. *IGFBP6* mRNA expression in 4 HCT116, MCF7, PC3 and CACO2 cells for 3h at 39°C compared to the same cell lines at 37°C. Bars represent the mean ± SEM of three different triplicate samples. Statistical comparisons were made using paired data Student' test. Difference were considered significant when $p < 0.05$.

6.4 IGFBP6 protein expression

We decided to study by flow cytometry the time course of IGFBP6 protein expression. In order to evaluate total and plasma membrane protein expression, the study was performed both on permeabilized (total protein, **Figure 12**) and non-permeabilized cells (expression on the plasma membrane, **Figure 13**).

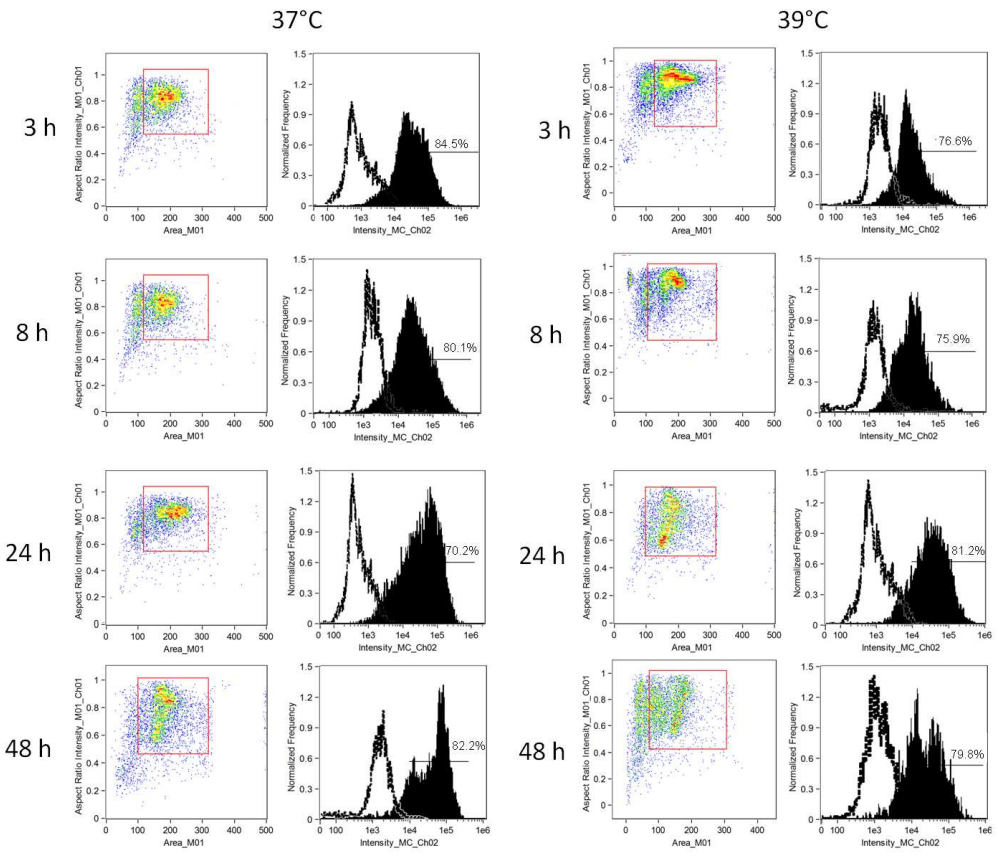

Figure 12. IGFBP6 expression in permeabilized moDCs. IGFBP6 expression was analyzed in moDCs after exposure for 3, 8, 24 and 48h at 39°C or for the same times at 37°C as controls. Cells were permeabilized and stained with an antibody anti-IGFBP6, followed by a secondary FITC antibody (black filled histograms). Histograms relative to the controls (cells stained only with secondary antibody) are shown with dotted lines. Gating strategy was performed considering scatter plots of control DCs at 37°C or 39°C obtained by plotting the Area vs. Aspect Ratio. Panels are representative of one case of the nine analyzed for gene expression.

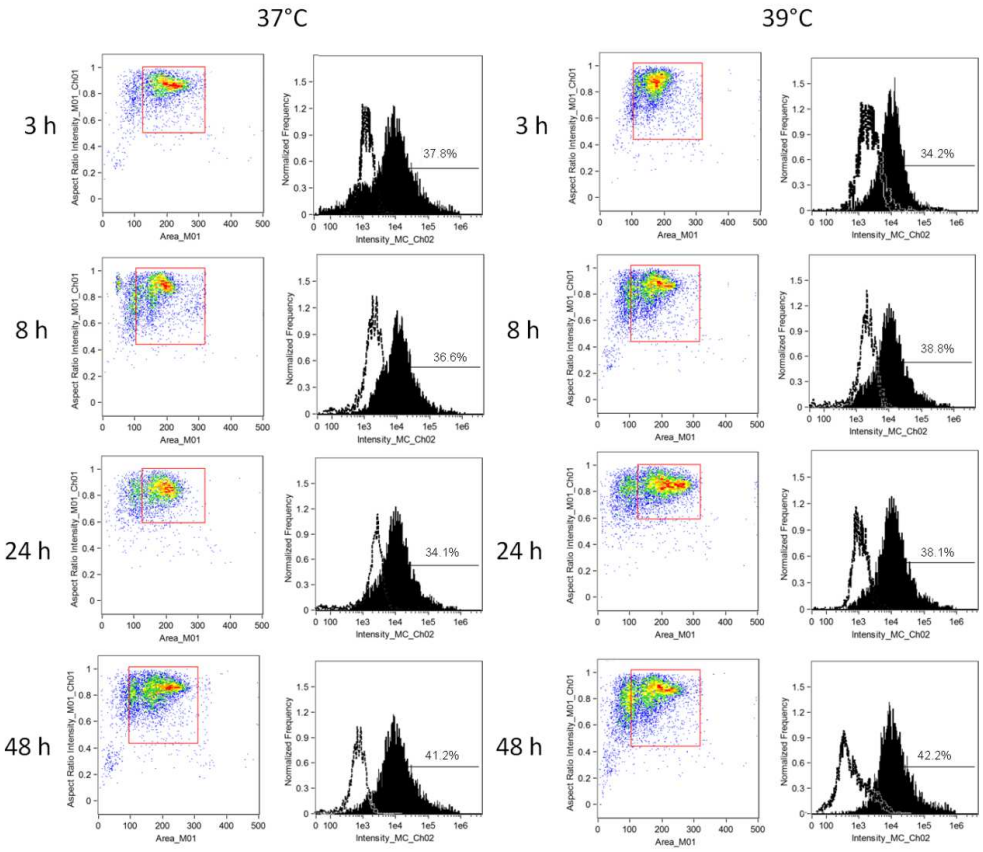

Figure 13. IGFBP6 expression in non-permeabilized moDCs. IGFBP6 expression was analyzed in moDCs after exposure for 3, 8, 24 and 48h at 39°C or for the same times at 37°C as controls. Cells were stained with an antibody anti-IGFBP6, followed by a secondary FITC antibody (black filled histograms). Histograms relative to the controls (cells stained only with secondary antibody) are shown with dotted lines. Gating strategy was performed considering scatter plots of control DCs at 37°C or 39°C obtained by plotting the Area vs. Aspect Ratio. Panels are representative of one case of the nine analyzed for gene expression.

Flow cytometry was performed with a specific monoclonal antibody (moAb) and showed that moDCs expressed detectable amounts of IGFBP6 both in permeabilized and non-permeabilized, when compared with cells stained with a control antibody. Permeabilized cells were gated in order to exclude the debris (**Figure 14A**) and the analysis was performed only on the gated populations. Data analysis showed that **~80% of permeabilized cells expressed IGFBP6** (**Figure 14C**). Moreover, **protein expression was independent of the temperature or exposure time**. While the percentage of cells expressing IGFBP6 was not influenced by the exposure time, the mean fluorescence intensity (**MFI**) **decreased after exposure at 39°C for 3 and 8 h** (**Figure 14D**). This pattern was reflected by the imaging of positive cells (**Figure 15**). Thus, the overall population remains positive for IGFBP6 at all time points (**Figure 13C**) but decreases its intracellular pool of the protein.

The same study was carried out in **non-permeabilized cells**. This condition did not alter cell viability (**Figure 14B**). Moreover, the number of cells **IGFBP6 positive was ~30% of total cells** (about 50% lower than the permeabilized cells) and was not affected by exposure at 39°C. Unlike permeabilized cells, **MFI was not significantly affected by exposure to hyperthermia** (**Figure 14F**). Individual cell imaging showed that IGFBP6 was expressed on the plasma membrane and that the expression did not change with temperature or exposure time (**Figure 15**).

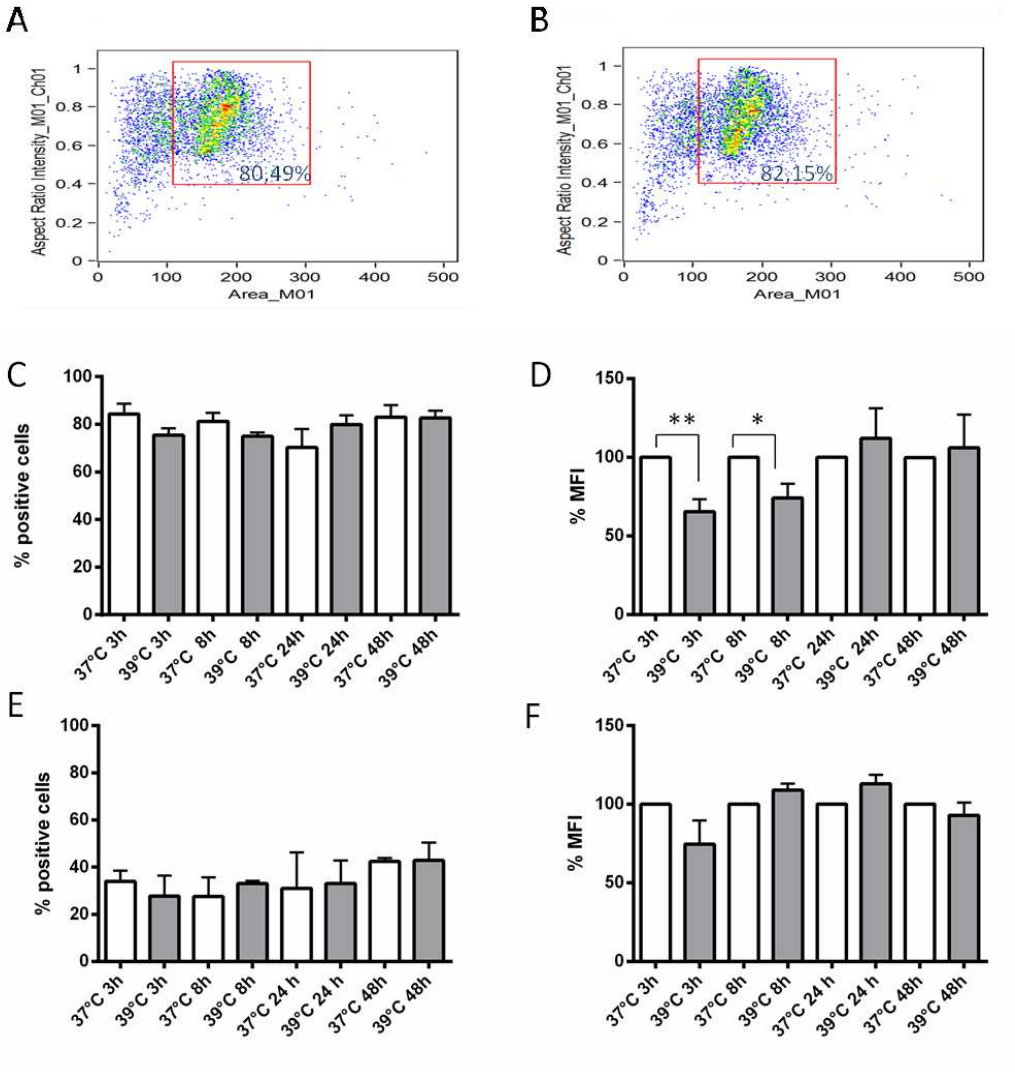

Figure 14. IGFBP6 expression levels in presence or absence of permeabilization. **A., B.** The dot plots, showing the typical distribution of DCs in presence (**A**) or in absence (**B**) of permeabilization. Permeabilization did not alter cell viability. **C., D., E., F.** Percentage of cells IGBP6^{+} after exposure for 3, 8, 24, and 48h at 39°C or at 37°C as controls and relative percentage of mean fluorescence intensity (MFI) of cells exposure at 39°C towards cells exposure at 37°C (considered as 100%) were analyzed in presence (**C** and **D**) or absence (**E** and **F**) of permeabilization. **C., D., E., F.** Bars represent mean ± SEM of four different samples. Statistical comparisons were made using unpaired Student' test. *p< 0.05, **p<0.001.

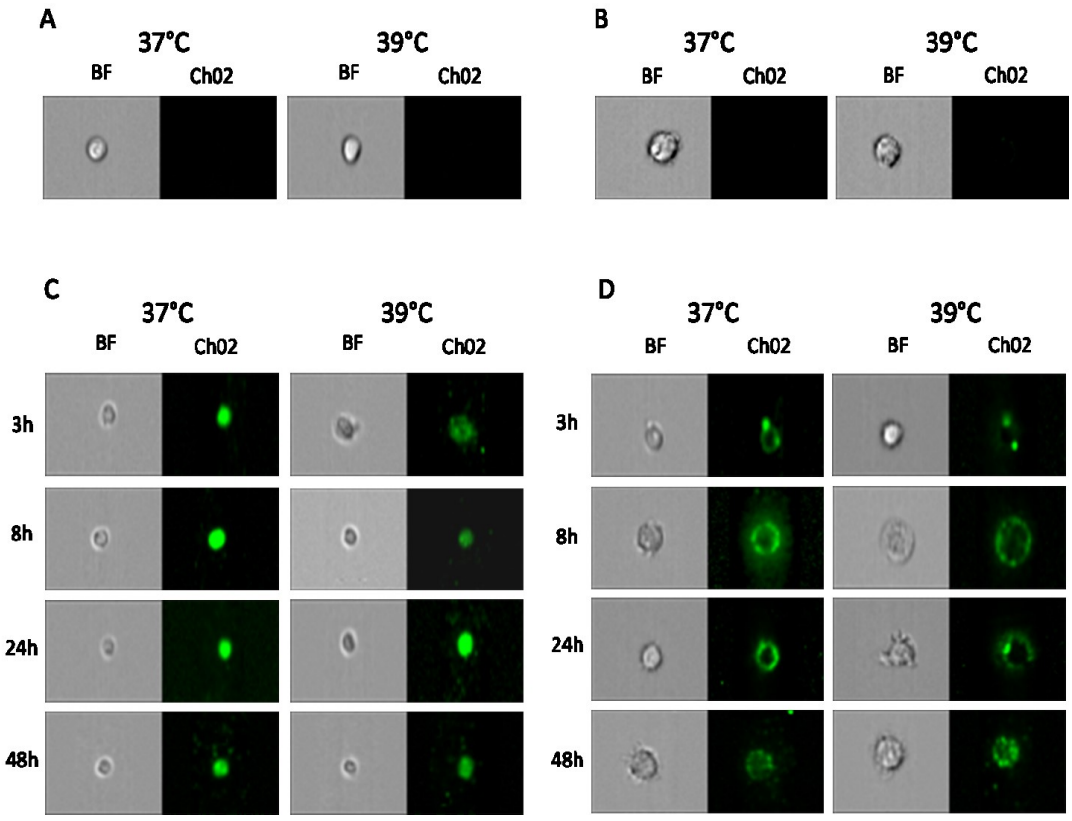

Figure 15. IGFBP6 expression in permeabilized and non-permeabilized DCs. Brightfield (BF) and green fluorescence images (Ch02) or single cells are shown. **A., B.** Negative controls were incubated only with FITC-conjugated secondary antibody (without anti-IGFBP6 primary antibody) in presence (**A**) or absence (**B**) of permeabilization. **C., D.** Cells were incubated with anti-IGFBP6 primary antibody and then with FITC-conjugated secondary antibody in presence (**C**) or absence (**D**) of permeabilization.

These data allowed us to conclude that **exposure to hyperthermia can reduce the pool of already synthesized protein** and hypothesize that IGFBP6 was secreted following exposure at 39°C. Then, we isolated the monocytes of nine healthy donors, induced differentiation into moDCs and after 6 days we replaced the culture medium. After exposure for 3, 8, 24 and 48 h at 39°C (or 37°C as a control) we collected the medium. Subsequently, we investigated the **secretion of IGFBP6** by immunological assay. IGFBP6 concentrations were **detectable only after 48 hours of exposure at 39°C** (**0.635 ± 0.023 ng/mL**), while the **secreted protein was never detectable at 37°C** (**Table 2**).

Incubation time	**IGFBP6 (ng/ml)**
37°C 3h	ND
39°C 3h	ND
37°C 8h	ND
39°C 8h	ND
37°C 24h	ND
39°C 24h	ND
37°C 48h	ND
39°C 48h	0,635±0,023

Table 2. IGFBP6 in conditioned medium. DCs were incubated at 39°C for different times (or at 37°C as controls). The IGFBP6 analysis was performed with the Milliplex technology (Millipore). ND: Not detectable.

We hypothesized that the secretion was coupled to apoptosis and/or necrosis. In order to confirm this hypothesis, we incubated moDCs for 3, 8, 24, and 48 h at 39°C (or 37°C as a control) and, after staining with Annexin V and 7-AAD, we investigated the pattern of apoptosis and necrosis. As a positive control, cells were incubated H_2O_2 for 24 h (**Table 3**) [168].

	Cell labeling (%)			
	$AnxV^-$ $7\text{-}AAD^-$	$AnxV^+$	$AnxV^+$ $7\text{-}AAD^+$	$7\text{-}AAD^+$
37°C	86.4±0.9	8.24±1.02	3.02±0.92	1.25±0.22
37°C+H_2O_2	70.0±0.05	17.35±0.55	6.60±0.20	6.04±0.05

Table 3. Effects of H_2O_2 on DCs viability. Dendritic cells were incubated in medium in presence or absence of H_2O_2 100 μM for 24 h and then evaluated by flow cyotmetry. Annexin V^+ ($AnxV^+$) corresponds to early apoptosis; AnV^+ $7\text{-}AAD^+$ staining to necrotic cells; $7\text{-}AAD^+$ staining to late apoptosis; AnV^- $7\text{-}AAD^+$ staining to healthy cells. Data are shown as mean ± SEM of three independent experiments.

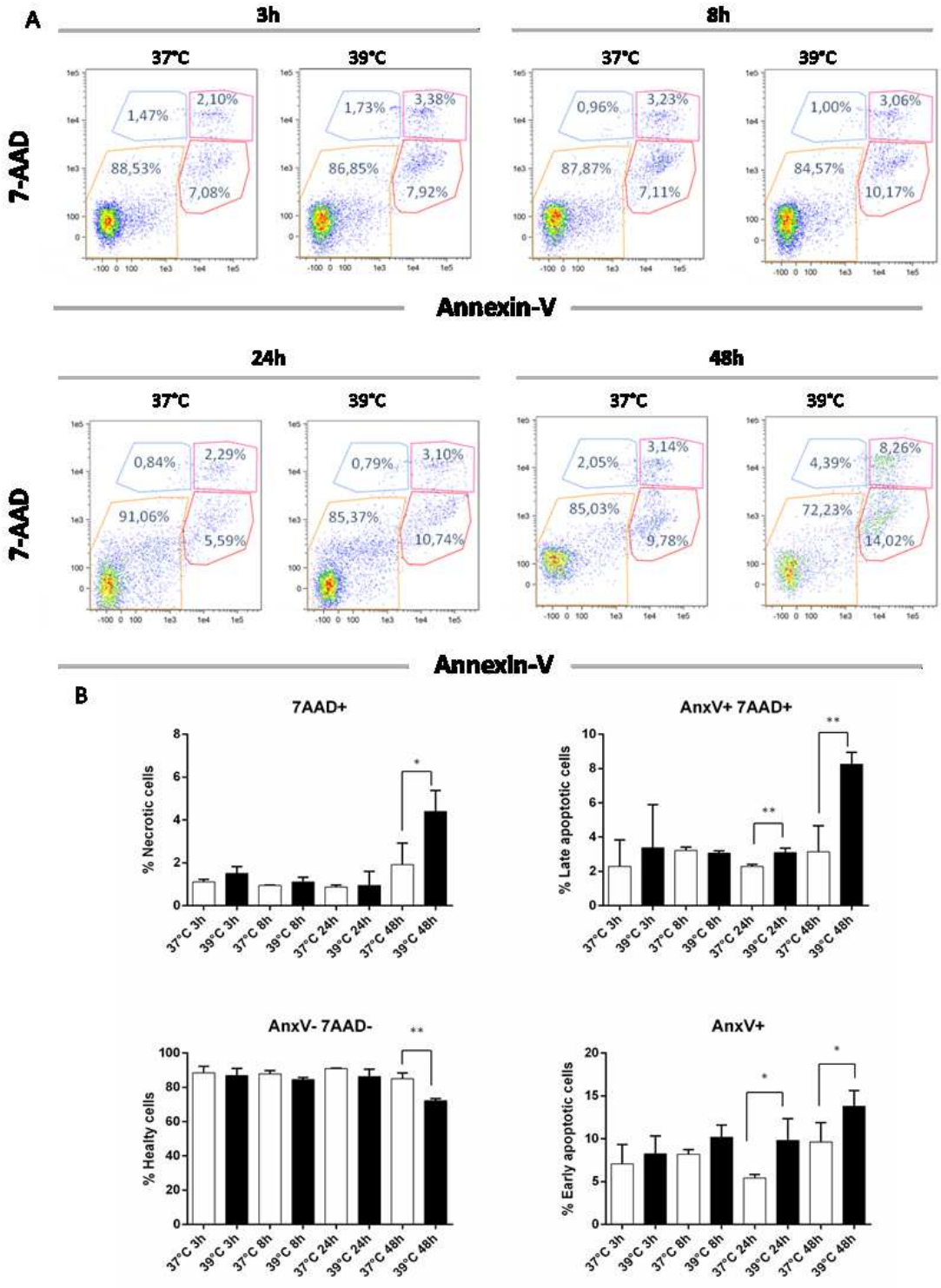

Figure 16. Apoptosis and necrosis after exposure at 39°C. moDCs were analyzed for apoptosis/necrosis after exposure at 39°C for 3, 8, 24, and 48h (or 37°C as controls). **A.,** Representative dot plots of moDCs after exposure to hyperthermic or normal conditions for different time points are shown. **B.,** The percentage of late apoptotic ($AnxV^-$ and $7AAD^+$), necrotic ($AnxV^+$ and $7AAD^+$), healthy ($AnxV^-$ and $7AAD^-$) and early apoptotic ($AnxV^+$ and $7AAD^-$) cells are shown as mean ± SEM of three independent experiments. Statistical comparisons were made using paired Student's *t* test. *$p< 0.05$, **$p<0.001$.

The data obtained showed a **different pattern of apoptosis and necrosis at 39°C** compared to 37°C (**Figure 16A**). DCs viability was ~85% at all time-points at 37°C and 39°C, except at 39°C for 48 h. After 48 hours of exposure at 39°C, the viability was around 70% (**Figure 16B**). Simultaneously, late apoptosis and necrosis ($AnxV^-/7AAD^+$ and $AnxV^+/7AAD^+$) were both suddenly increased after exposure at 39°C for 48 h, while early apoptosis ($AnxV^+/7AAD^-$) showed a more gradual increase in all time-points at 39°C. These data show that cell-associated **IGFBP6 expression decreases at early times after exposure at 39°C** and is followed by protein secretion. Furthermore, the decrease of DCs viability **at 39°C for 48 h**, coupled with an **increase in apoptosis/necrosis**, supports our hypothesis on the relationship between apoptosis/necrosis **and protein secretion**.

6.5 IGFBP6 is a chemoattractant factor in Monocytes and T cells but not in B cells

Based on the selective up-regulation of **IGFBP6** in moDCs, we hypothesized that this protein could play a **key role in immunity**. We therefore studied IGFBP6 as chemoattractant for monocytes, T lymphocytes and B lymphocytes by migration assay (Transwell, Corning). As a positive control, we used different concentrations of SDF-1 [86, 90, 116]. The data obtained showed that the addition of basolateral culture media with recombinant IGFBP6 increased the migration of both monocytes in a dose-dependent fashion to a maximum of 187 ± 31% of the control ($p<0.05$) (**Figure 17A**) both T cells, with a peak at 4 nM (0.1 μg/mL; 180 ± 29% of the control, $p<0.05$) (**Figure 17B**) but did not exert a significant chemotactic effect on B lymphocytes (**Figure 17C**). As shown in **Figure 17D**, the preincubation of IGFBP6 with an anti-IGFBP-6 antibody inhibited chemotactic function, whereas preincubation with an irrelevant antibody had a partial effect, as demonstrated by the statistically significant difference compared to the controls. Furthermore, we observed that Activin-A, an irrelevant mouse protein produced with the same system used for IGFBP6 and SDF-1 expression (insect cell culture infected with baculovirus) when used at the equivalent concentration, had no chemotactic effect (**Figure 17D**, **17E**, **17F**). These data show that **IGFBP6 has** an important **chemotactic effect on monocytes, T cells but not on B cells**, corroborating the hypothesis that this protein can play a crucial role in the immune system.

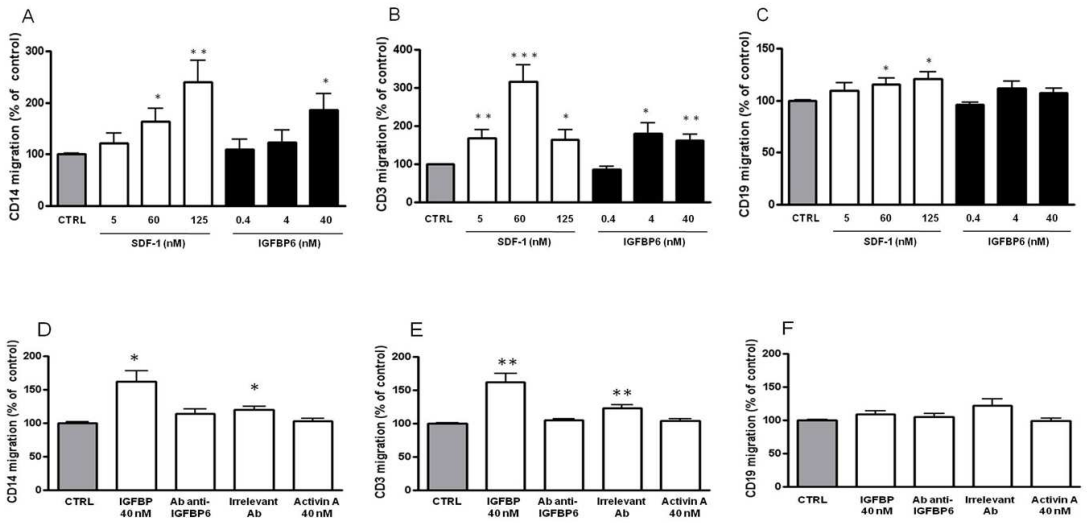

Figure 17. Chemoattractive effect of IGFBP6 on monocytes, T cells and B cells. **A., B., C.** Monocytes (**A**), T lymphocytes (**B**) and B lymphocytes (**C**) were placed in the upper compartment of a Transwell with or without IGFBP6 at the different concentrations (0.4 nM, 4 nM, 40nM) in the lower compartment. Number of migrating cells through a 3µm-pore membrane was measured by flow cytometry. Positive control: different concentrations of SDF-1 (5 nM, 60 nM, 125 nM) in the lower compartment were used. Results are shown as mean ± SEM of three independent experiments and expressed as a percentage of controls (absence of IGFBP6 in the basolateral compartment) and set at 100%. *p< 0.05, **p<0.001, ***p<0.0001. **D., E., F.** Monocytes (**D**), T lymphocytes (**E**), B lymphocytes (**F**) were placed in the upper compartment of Transwell in the presence in the lower compartment of IGFBP6 40 nM; IGFBP6 40 nM pre-incubated with an antibody direct against IGFBP6; IGFBP6 40 nM pre-incubated with an irrelevant antibody, Activin A 40 nM as a negative control. Results are shown as mean ±SEM of three independent experiments and expressed as a percentage of controls (absence of IGFBP6 in the basolateral compartment) and set at 100%. *p< 0.05, **p<0.001, ***p<0.0001. **A., B., C., D., E., F.** Results were analyzed using 2-way ANOVA with Turkey's Multiple Comparison test.

6.6 Neutrophils during inflammation: IGFBP6 and ROS production

Based on the important function exercised by IGFBP6 on DCs, we decided to explore the role of this protein in neutrophil activity during inflammation. First of all, we tested the possible generation of intracellular reactive oxygen species (ROS). Cells were treated with different concentrations of IGFBP6 and ROS production was evaluated by the peroxisensitive fluorescent probe DCF. Data were acquired by flow cytometry [169]. The data obtained showed that IGFBP6 induces a significant increase in ROS production at all concentrations tested (compared to untreated control), with a peak at 1 μg/mL (**Figure 18A**). Starting from this result we decided to investigate if IGFBP6 may increase or potentiate other stimuli. Thus, neutrophils were incubated with IGFBP6 and then with fMLP or PMA. As shown in **Figure 18B**, neutrophils stimulated with fMLP or PMA after incubation with IGFBP6 showed no difference in ROS generation compared to neutrophils incubated with fMLP or PMA only. Our study showed that **IGFBP6 increases oxidative burst in neutrophils** (with a peak obtained at 1 μg/mL) **and has no priming effect.**

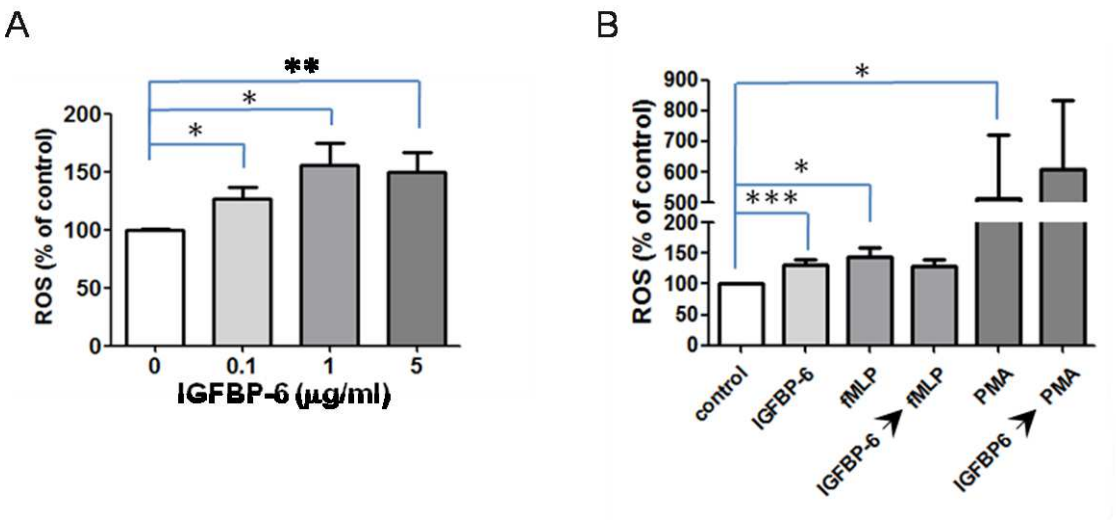

Figure 18. IGFBP6 and ROS production. A. Neutrophils were incubated with IGFBP6 at different concentrations (0.1µg/ml, 1µg/ml and 5 µg/ml) for 50 min and then with DCF probe for 10 min. The percentages of ROS production were analyzed by flow cytometry. Results are shown as mean ± SEM of five-seven independent experiments and expressed as a percentage of controls and set at 100%. *p< 0.05, **p<0.001, ***p<0.0001. **B.** Neutrophils were incubated with: IGFBP6 1µg/ml; fMLP 1µM; pre-incubated with IGFBP6 1µg/ml and then with fMLP 1µM; PMA 10nM; pre-incubated with IGFBP6 1µg/ml and then with PMA 10nM. After these incubations, cultured moDCs were supplemented with DCF and visualized by flow cytometry. Results are shown as mean ± SEM of seven independent experiments and expressed as a percentage of controls and set at 100%. *p< 0.05, **p<0.001, ***p<0.0001. **A., B.** As a control, experiments were conducted in the absence of IGFBP6. Statistical comparisons were made using unpaired Student's *t* test.

6.7 Neutrophils during inflammation: IGFBP6 and degranulation

Subsequently, we investigated the role of IGFBP6 in granule release. Degranulation was studied in terms of release of myeloperoxidase (MPO, primary granules) and metalloproteinase-9 (MMP-9, tertiary granules) by ELISA. As a positive control, we used fMLP which significantly increased primary and tertiary granule secretion (**Figure 19**), whereas TNF-α was ineffective (data not shown). The data obtained showed that IGFBP6 was able to increase MPO levels (**Figure 19A**) but did not modify MMP-9 levels (**Figure 19B**) as compared with controls. Moreover, MPO and MMP-9 levels did not modify by pre-incubating neutrophils with IGFBP6 and then with fMLP. Also in this case, data obtained showed that neutrophils pre-incubated with IGFBP6 prior to stimulation with fMLP did not shown any difference as compared with neutrophils incubated with fMLP only. We can conclude that **IGFBP6 increases MPO levels but does not modify MMP-9 levels and has no priming effect.**

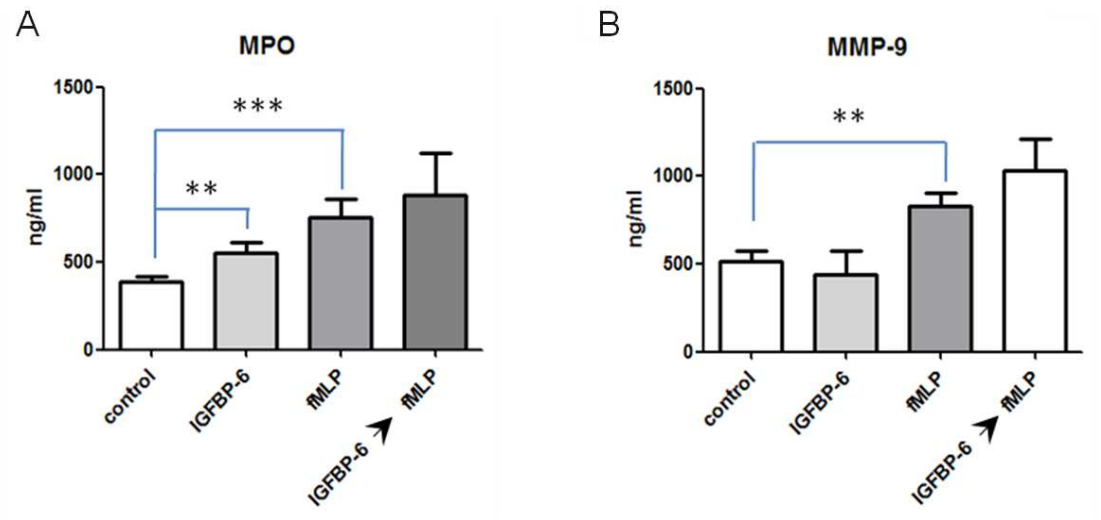

Figure 19. IGFBP6 and degranulation. A., B. Neutrophils were incubated with: IGFBP6 1µg/ml; fMLP 1µM; pre-incubated with IGFBP6 1µg/ml and then with fMLP 1µM.The Neutrophils supernatant was collected and the (**A**) MPO or (**B**) MMP-9 content was assessed by ELISA test. The values in the histogram are mean ± SEM of five-seven independent experiments and carried out in triplicate experimental replicates under each condition. **p*< 0.05, ***p*<0.001, ****p*<0.0001. **A., B.** Statistical comparisons were made using unpaired Student's *t* test.

6.8 Neutrophils during inflammation: IGFBP6 and chemotaxis

Finally, IGFBP6 was studied as chemotactic agent in a polarized model of airway epithelium in physiologically relevant mode. Thus, we added neutrophils to the basolateral side of the epithelium and IGFBP6 to the apical side. As shown in **Figure 20A**, IGFBP6 induces chemotaxis in neutrophils (peak at 0.1 and 1 μg/mL), although less than fMLP. Also in this case we studied whether the protein could have a priming effect by pre-incubating neutrophils with 1 μg/ml of IGFBP6. Thus, after incubation with IGFBP6, cells were added to the basolateral side of the epithelium in the presence of apical fMLP. The percentage of neutrophils that transmigrated did not differ from those untreated (**Figure 20B**). Data show **that IGFBP6 induces chemotaxis in neutrophils but does not exert the priming effect**.

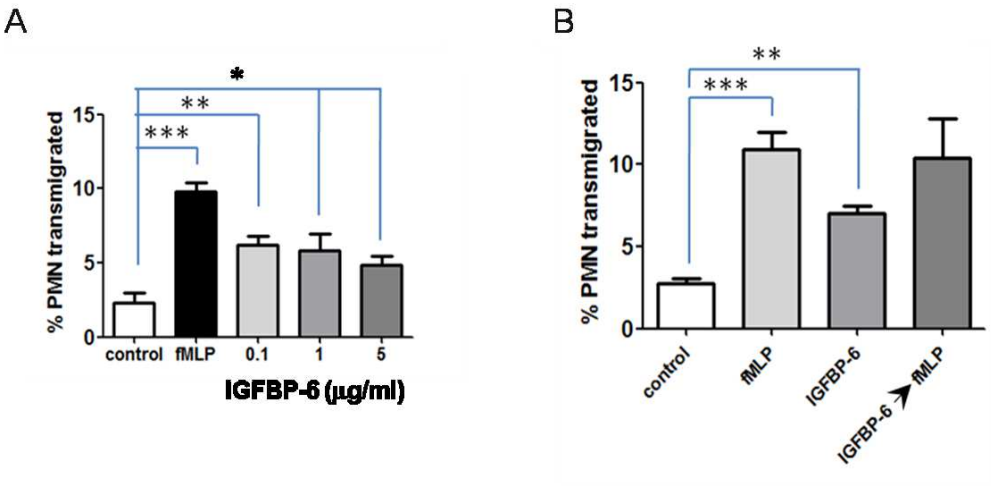

Figure 20. Chemoattractive effect of IGFBP6 on neutrophils. A. Neutrophils were placed in the basolateral side of Transwell in absence or presence of IGFBP6 at different concentrations (0.1µg/ml, 1µg/ml and 5µg/ml) in the apical compartment. Number of migrating cells through the epithelial monolayer was measured by flow cytometry. Positive control: fMLP 1 µM in the lower compartment was used. Results are shown as mean ± SEM of seven independent experiments and expressed as a percentage of controls. **p*< 0.05, ***p*<0.001, ****p*<0.0001. **B.** Neutrophils were placed in the basolateral compartment in the presence in the apical compartment of: IGFBP6 1µg/ml; fMLP 1µM; pre-incubated with IGFBP6 1µg/ml for 50 minutes and then placed in the basolateral side of the epithelium in the presence of apical fMLP 1µM. Results are shown as mean ± SEM of seven independent experiments and expressed as a percentage of controls. **p*< 0.05, ***p*<0.001, ****p*<0.0001. **A., B.** Statistical comparisons were made using unpaired Student's *t* test.

7. Discussion

The role of immune system in eradicating malignant cells is not yet fully understood, however it has been shown that the regression of some cancers is associated with induction of fever and activation of the immune system [170, 171]. Fever, and therefore hyperthermia, can be a highly effective cancer treatment, especially if associated with other therapies such as chemotherapy, radiotherapy and immunotherapy [172, 173]. Several studies have shown that monocytes, besides acting as precursors of macrophages, have the capacity to differentiate into DCs, and therefore play an important role in innate and adaptive immunity.

The present study investigated in depth the effect of fever-like temperatures (also known as hyperthermia) on gene expression programs in myeloid DCs generated *in vitro* from monocytes as a defined starting cell population. The results obtained show that primary dendritic cells derived from human monocytes exhibit thermo-sensitivity. This thermo-sensitivity has been highlighted in terms of maturation and up- or down- regulation of gene expression profile. It is known that, both murine and human monocytes when cultured with GM-CSF and IL-4, differentiate into immature monocyte derived-dendritic cells (immature moDCs) [174].

Moreover, a study shows that exposure of moDCs at 40°C induces an increased expression of the costimulatory molecules and therefore maturation of these cells [26]. Starting from these data, we have shown that exposure for 24 h at 39°C may enhance the function and immunostimulatory property of human moDCs. Numerous mechanism have been proposed by which fever can confer protection, among them, the best known are the following, by killing or inhibiting growth of pathogens; inducing cytoprotective HSPs in host cells; inducing activation of host defeses by the expression of pathogenic HSPs; or by modifying and modulating the host's defenses directly [175-177]. This study has highlighted the central role of the heat shock response in the process of DC maturation. We decided to explore the global gene expression profile of DCs in order to understand which genes were up- and down-regulated (Table 1). As expected, among the up-regulated genes, there were HSPs, such as HSP90. HSPs are involved in a myriad of immune modulation functions, for example, HSP60, HSP70 and HSP90 have been proposed to play a critical role in antigen presentation and DC activation [178]. These HSPs are implicated in immunomodulation [179]. Indeed, Hsp60 is associated with T1DM because it

induces both pro-inflammatory and anti-inflammatory cytokines. It binds multiple allelic variants of HLA-DR, resulting in the release of an anti-inflammatory cytokine, such as IL-1, and IFN-γ [180]. This HSP is also associated with T2DM, since, the interaction of Hsp60 with TL2 and TLR4 leads to release of pro-inflammatory cytokines, such as IL-1, IL-6, IL-8, MCP-1 and TNF-α [181]. Instead, Hsp70 promotes the production of anti-inflammatory cytokines; interact with DCs, MDSCs, and monocytes, binding to their endocytic receptors resulting in the release of anti-inflammatory cytokine IL-10 and immunosuppression in chronic inflammatory diseases [182], while, in cancer, it acts as an extracellular recognition site for NK cells [183]. Finally, Hsp90 is implicated in T-cell mediated anti-tumor responses, in fact, Hsp90 inhibition up-regulates expression of interferon response genes, which promotes the killing of melanoma cells by T cells [184].

In addition to these genes, it was intriguing that a few up-regulated genes encoded secreted proteins, namely *MANF*, *PLAT*, and *IGFBP6*. We have focused our attention only on these proteins by assuming that a secreted protein is a protein potentially capable of interacting with other immune cells through receptors. We showed that up-regulation after exposure of DCs to hyperthermia is consistent and significant only in *IGFBP6*. We have shown that *IGFBP6* is specific to DCs, since this gene is not up-regulated in ontogenetically distant cell lines (epithelial cell lines) or monocytes. Up-regulation would appear to be a distinct feature that dendritic cells acquire when they mature from monocytes.

Considering the up-regulation of the *IGFBP6* gene after exposure at 39°C for 3h, we focused our attention on the consequences of this increase at the protein level. Furthermore, intracellular staining did not show an increase in protein levels after exposure at 39°C but a significant decrease up to 8 h with a later increase at 24 and 48 hours, whereas membrane-bound staining was only slightly decreases at 3 hours. These data indicate that up-regulation of the *IGFBP6* gene is not related by a linear increase in protein expression and suggest that the decrease of intracellular IGFBP6 could be recovered by subsequent synthesis.

We have shown that the decrease in cellular protein was not associated with the appearance of protein in the conditioned medium, but required 48 h of exposure at 39°C. We therefore hypothesized that IGFBP6 was secreted as a result of cell damage phenomena. Thus, we investigated whether IGFBP6 secretion was linked to necrosis, finding that it was indeed so. In addition to well-known functions of

IGFBP6, such as inhibition of IGF-II, proliferation, migration and differentiation of numerous cell lines [86], recent studies suggest that IGFBP6 acts as a chemotactic agent. Indeed, IGFBP6 (40 nM, 1μg/ml) has a chemoattractant action for both Rh30 rabdomyosarcoma cells [116] and for RA immune cells, in particular T lymphocytes, and this effect is partially inhibited by dexamethasone [153]. Therefore, we examined the possible chemotactic ability of IGFBP6 in regard to freshly isolated peripheral lymphocytes and monocytes. We have shown that IGFBP6 induces chemotaxis of monocytes and T cells, nut not of B cells. Furthermore, the chemoattractant effect was observed at about 150-fold higher concentrations than those found in the conditioned medium. These data allow us to hypothesize that secretion of IGFBP6 during exposure at 39°C can mediate dendritic cells-T lymphocytes encounters.

Starting from data obtained on DCs, we decided to explore the action of IGFBP6 protein in neutrophil activities during inflammation. IGFBP6 has been studied in terms of ROS production, granule release and chemotaxis in a model that mimicking the airway epithelium. Our data show that IGFBP6 does not act as priming in neutrophils but activates neutrophils already activated by other inflammatory stimuli. It is known that the generation of ROS by neutrophils plays a key role in the degradation of bacteria and therefore in the protection of the host [185].

In this regard, we investigated the role of IGFBP6 in the oxidative burst and found that IGFBP6 induces a significant increase in ROS production.

One of the peculiar characteristics of neutrophils is granular exocytosis and release of their cytotoxic contents on the plasma membrane. Neutrophil granules contain numerous antimicrobial and cytotoxic substances that are delivered to the phagosome or to the exterior of the cell after degranulation [186]. Among the most important enzymes released during activation, there are myeloperoxidase (MPO) and metalloproteinase-9 (MMP-9). Thus, we studied degranulation in terms of release of MPO and MMP-9 and we found that IGFBP6 increased significantly MPO levels (primary granules), but did not modify MMP-9 levels (tertiary granules). Finally, considering the data we obtained on the chemotaxis in T cells and monocytes and considering the data in Rh30 rabdomyosarcoma cells [116] and in RA immune cells [153], we have tested this activity in neutrophils. Surprisingly, the chemotactic function of IGFBP6 was also exerted in neutrophils (with a peak at 1 μg/mL).

8. Conclusion

In summary, by analyzing the gene expression profiles of human moDCs from nine healthy donors, we found that a mild hyperthermia (3h at 39°C) induces changes in the metabolic phenotype and alteration of gene expression profile, with an up-down regulation of some genes: up-regulation of 43 genes and down-regulation of 24 genes. Some of the up-regulated genes encode for secreted proteins (*IGFBP6*, *MANF* and *PLAT*). In particular, in moDCs hyperthermia induces apoptosis and necrosis with a concomitant secretion of IGFBP6. Furthermore, IGFBP6 induces chemotaxis of monocytes and T lymphocytes, but not B lymphocytes. Finally, we have analyzed the behavior of neutrophils when stimulated with IGFBP6. Also, in this case, IGFBP6 has shown an important role since it is involved in ROS production, degranulation and migration through the epithelial monolayer.

In conclusion, IGFBP6 appears to play a key role in controlling the immunological adaptation of cells after hyperthermia and is a factor capable of inducing selective chemotaxis. Considering the consistency of the data obtained, it would be necessary to test both the ability of other DCs subtypes to secrete IGFBP6 and the behavior of the different T cells subtypes when exposed to IGFBP6.

Furthermore, other studies should be made to clarify which signaling pathways are activated by IGFBP6 in neutrophils.

In vivo studies are needed to explore the role of IGFBP6 in cancer and immune pathologies and to discover the potential of this protein in diagnosis and therapy.

9. ReferencesREFERENCES

1. Kluger MJ. Phylogeny of fever. *Fed Proc* 38(1), 30-34 (1979).
2. Earn DJ, Andrews PW, Bolker BM. Population-level effects of suppressing fever. *Proc Biol Sci* 281(1778), 20132570 (2014).
3. Maclaren G SD. Fever in the intensive care unit. *UpToDate* (2017).
4. O'grady NP, Barie PS, Bartlett JG *et al*. Guidelines for evaluation of new fever in critically ill adult patients: 2008 update from the American College of Critical Care Medicine and the Infectious Diseases Society of America. *Crit Care Med* 36(4), 1330-1349 (2008).
5. Akira S, Takeda K. Toll-like receptor signalling. *Nat Rev Immunol* 4(7), 499-511 (2004).
6. Hasday JD, Thompson C, Singh IS. Fever, immunity, and molecular adaptations. *Compr Physiol* 4(1), 109-148 (2014).
7. Cao C, Matsumura K, Yamagata K, Watanabe Y. Endothelial cells of the rat brain vasculature express cyclooxygenase-2 mRNA in response to systemic interleukin-1 beta: a possible site of prostaglandin synthesis responsible for fever. *Brain Res* 733(2), 263-272 (1996).
8. Konsman JP, Vigues S, Mackerlova L, Bristow A, Blomqvist A. Rat brain vascular distribution of interleukin-1 type-1 receptor immunoreactivity: relationship to patterns of inducible cyclooxygenase expression by peripheral inflammatory stimuli. *J Comp Neurol* 472(1), 113-129 (2004).
9. Matsumura K, Cao C, Ozaki M, Morii H, Nakadate K, Watanabe Y. Brain endothelial cells express cyclooxygenase-2 during lipopolysaccharide-induced fever: light and electron microscopic immunocytochemical studies. *J Neurosci* 18(16), 6279-6289 (1998).
10. Yamagata K, Matsumura K, Inoue W *et al*. Coexpression of microsomal-type prostaglandin E synthase with cyclooxygenase-2 in brain endothelial cells of rats during endotoxin-induced fever. *J Neurosci* 21(8), 2669-2677 (2001).
11. Engstrom L, Ruud J, Eskilsson A *et al*. Lipopolysaccharide-induced fever depends on prostaglandin E2 production specifically in brain endothelial cells. *Endocrinology* 153(10), 4849-4861 (2012).
12. Romanovsky AA. Thermoregulation: some concepts have changed. Functional architecture of the thermoregulatory system. *Am J Physiol Regul Integr Comp Physiol* 292(1), R37-46 (2007).
13. Morrison SF, Madden CJ, Tupone D. Central control of brown adipose tissue thermogenesis. *Front Endocrinol (Lausanne)* 3(5), (2012).
14. Nakamura K, Morrison SF. A thermosensory pathway that controls body temperature. *Nat Neurosci* 11(1), 62-71 (2008).
15. Dantzer R, Wollman E. Molecular mechanisms of fever: the missing links. *Eur Cytokine Netw* 9(1), 27-31 (1998).
16. Soehnlein O, Lindbom L. Phagocyte partnership during the onset and resolution of inflammation. *Nat Rev Immunol* 10(6), 427-439 (2010).
17. Toussaint E, Bahel-Ball E, Vekemans M *et al*. Causes of fever in cancer patients (prospective study over 477 episodes). *Support Care Cancer* 14(7), 763-769 (2006).
18. Chang JC, Gross HM. Neoplastic fever responds to the treatment of an adequate dose of naproxen. *J Clin Oncol* 3(4), 552-558 (1985).
19. Zell JA, Chang JC. Neoplastic fever: a neglected paraneoplastic syndrome. *Support Care Cancer* 13(11), 870-877 (2005).
20. Pasikhova Y, Ludlow S, Baluch A. Fever in Patients With Cancer. *Cancer Control* 24(2), 193-197 (2017).
21. Patel RA, Gallagher JC. Drug fever. *Pharmacotherapy* 30(1), 57-69 (2010).
22. Hanson DF. Fever, temperature, and the immune response. *Ann N Y Acad Sci* 813 453-464 (1997).
23. Park HG, Han SI, Oh SY, Kang HS. Cellular responses to mild heat stress. *Cell Mol Life Sci* 62(1), 10-23 (2005).
24. Hatzfeld-Charbonnier AS, Lasek A, Castera L *et al*. Influence of heat stress on human monocyte-derived dendritic cell functions with immunotherapeutic potential for antitumor vaccines. *J Leukoc Biol* 81(5), 1179-1187 (2007).
25. Diaz FE, Dantas E, Cabrera M *et al*. Fever-range hyperthermia improves the anti-apoptotic effect induced by low pH on human neutrophils promoting a proangiogenic profile. *Cell Death Dis* 7(10), e2437 (2016).

26. Knippertz I, Stein MF, Dorrie J *et al*. Mild hyperthermia enhances human monocyte-derived dendritic cell functions and offers potential for applications in vaccination strategies. *Int J Hyperthermia* 27(6), 591-603 (2011).
27. Chen DS, Mellman I. Oncology meets immunology: the cancer-immunity cycle. *Immunity* 39(1), 1-10 (2013).
28. Mildner A, Jung S. Development and function of dendritic cell subsets. *Immunity* 40(5), 642-656 (2014).
29. Villadangos JA, Heath WR. Life cycle, migration and antigen presenting functions of spleen and lymph node dendritic cells: limitations of the Langerhans cells paradigm. *Semin Immunol* 17(4), 262-272 (2005).
30. Siegal FP, Kadowaki N, Shodell M *et al*. The nature of the principal type 1 interferon-producing cells in human blood. *Science* 284(5421), 1835-1837 (1999).
31. Asselin-Paturel C, Boonstra A, Dalod M *et al*. Mouse type I IFN-producing cells are immature APCs with plasmacytoid morphology. *Nat Immunol* 2(12), 1144-1150 (2001).
32. Swiecki M, Colonna M. The multifaceted biology of plasmacytoid dendritic cells. *Nat Rev Immunol* 15(8), 471-485 (2015).
33. Serbina NV, Salazar-Mather TP, Biron CA, Kuziel WA, Pamer EG. TNF/iNOS-producing dendritic cells mediate innate immune defense against bacterial infection. *Immunity* 19(1), 59-70 (2003).
34. Mildner A, Yona S, Jung S. A close encounter of the third kind: monocyte-derived cells. *Adv Immunol* 120 69-103 (2013).
35. Segura E, Amigorena S. Inflammatory dendritic cells in mice and humans. *Trends Immunol* 34(9), 440-445 (2013).
36. Plantinga M, Guilliams M, Vanheerswynghels M *et al*. Conventional and monocyte-derived CD11b(+) dendritic cells initiate and maintain T helper 2 cell-mediated immunity to house dust mite allergen. *Immunity* 38(2), 322-335 (2013).
37. Tamoutounour S, Henri S, Lelouard H *et al*. CD64 distinguishes macrophages from dendritic cells in the gut and reveals the Th1-inducing role of mesenteric lymph node macrophages during colitis. *Eur J Immunol* 42(12), 3150-3166 (2012).
38. Sallusto F, Lanzavecchia A. Efficient presentation of soluble antigen by cultured human dendritic cells is maintained by granulocyte/macrophage colony-stimulating factor plus interleukin 4 and downregulated by tumor necrosis factor alpha. *J Exp Med* 179(4), 1109-1118 (1994).
39. Banchereau J, Briere F, Caux C *et al*. Immunobiology of dendritic cells. *Annu Rev Immunol* 18 767-811 (2000).
40. Rescigno M, Granucci F, Citterio S, Foti M, Ricciardi-Castagnoli P. Coordinated events during bacteria-induced DC maturation. *Immunol Today* 20(5), 200-203 (1999).
41. Akbari O, Panjwani N, Garcia S, Tascon R, Lowrie D, Stockinger B. DNA vaccination: transfection and activation of dendritic cells as key events for immunity. *J Exp Med* 189(1), 169-178 (1999).
42. Hacker H, Mischak H, Miethke T *et al*. CpG-DNA-specific activation of antigen-presenting cells requires stress kinase activity and is preceded by non-specific endocytosis and endosomal maturation. *EMBO J* 17(21), 6230-6240 (1998).
43. Hartmann G, Weiner GJ, Krieg AM. CpG DNA: a potent signal for growth, activation, and maturation of human dendritic cells. *Proc Natl Acad Sci U S A* 96(16), 9305-9310 (1999).
44. Cella M, Salio M, Sakakibara Y, Langen H, Julkunen I, Lanzavecchia A. Maturation, activation, and protection of dendritic cells induced by double-stranded RNA. *J Exp Med* 189(5), 821-829 (1999).
45. Mosialos G, Birkenbach M, Ayehunie S *et al*. Circulating human dendritic cells differentially express high levels of a 55-kd actin-bundling protein. *Am J Pathol* 148(2), 593-600 (1996).
46. Winzler C, Rovere P, Rescigno M *et al*. Maturation stages of mouse dendritic cells in growth factor-dependent long-term cultures. *J Exp Med* 185(2), 317-328 (1997).
47. Ng YH, Chalasani G. Role of secondary lymphoid tissues in primary and memory T-cell responses to a transplanted organ. *Transplant Rev (Orlando)* 24(1), 32-41 (2010).
48. Mullins DW, Sheasley SL, Ream RM, Bullock TN, Fu YX, Engelhard VH. Route of immunization with peptide-pulsed dendritic cells controls the distribution of memory and effector T cells in lymphoid tissues and determines the pattern of regional tumor control. *J Exp Med* 198(7), 1023-1034 (2003).
49. Cavanagh LL, Bonasio R, Mazo IB *et al*. Activation of bone marrow-resident memory T cells by circulating, antigen-bearing dendritic cells. *Nat Immunol* 6(10), 1029-1037 (2005).

50. Bonasio R, Scimone ML, Schaerli P, Grabie N, Lichtman AH, Von Andrian UH. Clonal deletion of thymocytes by circulating dendritic cells homing to the thymus. *Nat Immunol* 7(10), 1092-1100 (2006).
51. Gardner A, Ruffell B. Dendritic Cells and Cancer Immunity. *Trends Immunol* 37(12), 855-865 (2016).
52. Roberts EW, Broz ML, Binnewies M *et al*. Critical Role for CD103(+)/CD141(+) Dendritic Cells Bearing CCR7 for Tumor Antigen Trafficking and Priming of T Cell Immunity in Melanoma. *Cancer Cell* 30(2), 324-336 (2016).
53. Hanahan D, Weinberg RA. Hallmarks of cancer: the next generation. *Cell* 144(5), 646-674 (2011).
54. O'neill LA, Pearce EJ. Immunometabolism governs dendritic cell and macrophage function. *J Exp Med* 213(1), 15-23 (2016).
55. Mills EL, O'neill LA. Reprogramming mitochondrial metabolism in macrophages as an anti-inflammatory signal. *Eur J Immunol* 46(1), 13-21 (2016).
56. Liso A, Capitanio N, Gerli R, Conese M. From fever to immunity: A new role for IGFBP-6? *J Cell Mol Med* 22(10), 4588-4596 (2018).
57. Menga M, Trotta R, Scrima R *et al*. Febrile temperature reprograms by redox-mediated signaling the mitochondrial metabolic phenotype in monocyte-derived dendritic cells. *Biochim Biophys Acta Mol Basis Dis* 1864(3), 685-699 (2018).
58. Silva MT, Correia-Neves M. Neutrophils and macrophages: the main partners of phagocyte cell systems. *Front Immunol* 3 174 (2012).
59. Hachicha M, Naccache PH, Mccoll SR. Inflammatory microcrystals differentially regulate the secretion of macrophage inflammatory protein 1 and interleukin 8 by human neutrophils: a possible mechanism of neutrophil recruitment to sites of inflammation in synovitis. *J Exp Med* 182(6), 2019-2025 (1995).
60. Borregaard N. Neutrophils, from marrow to microbes. *Immunity* 33(5), 657-670 (2010).
61. Mantovani A, Cassatella MA, Costantini C, Jaillon S. Neutrophils in the activation and regulation of innate and adaptive immunity. *Nat Rev Immunol* 11(8), 519-531 (2011).
62. Nathan C. Neutrophils and immunity: challenges and opportunities. *Nat Rev Immunol* 6(3), 173-182 (2006).
63. Sheshachalam A, Srivastava N, Mitchell T, Lacy P, Eitzen G. Granule protein processing and regulated secretion in neutrophils. *Front Immunol* 5 448 (2014).
64. Coffelt SB, Wellenstein MD, De Visser KE. Neutrophils in cancer: neutral no more. *Nat Rev Cancer* 16(7), 431-446 (2016).
65. Jamieson T, Clarke M, Steele CW *et al*. Inhibition of CXCR2 profoundly suppresses inflammation-driven and spontaneous tumorigenesis. *J Clin Invest* 122(9), 3127-3144 (2012).
66. Templeton AJ, Mcnamara MG, Seruga B *et al*. Prognostic role of neutrophil-to-lymphocyte ratio in solid tumors: a systematic review and meta-analysis. *J Natl Cancer Inst* 106(6), dju124 (2014).
67. Swierczak A, Mouchemore KA, Hamilton JA, Anderson RL. Neutrophils: important contributors to tumor progression and metastasis. *Cancer Metastasis Rev* 34(4), 735-751 (2015).
68. Gregory AD, Houghton AM. Tumor-associated neutrophils: new targets for cancer therapy. *Cancer Res* 71(7), 2411-2416 (2011).
69. Tecchio C, Scapini P, Pizzolo G, Cassatella MA. On the cytokines produced by human neutrophils in tumors. *Semin Cancer Biol* 23(3), 159-170 (2013).
70. Fridlender ZG, Sun J, Kim S *et al*. Polarization of tumor-associated neutrophil phenotype by TGF-beta: "N1" versus "N2" TAN. *Cancer Cell* 16(3), 183-194 (2009).
71. Bodogai M, Moritoh K, Lee-Chang C *et al*. Immunosuppressive and Prometastatic Functions of Myeloid-Derived Suppressive Cells Rely upon Education from Tumor-Associated B Cells. *Cancer Res* 75(17), 3456-3465 (2015).
72. Costantini C, Micheletti A, Calzetti F, Perbellini O, Pizzolo G, Cassatella MA. Neutrophil activation and survival are modulated by interaction with NK cells. *Int Immunol* 22(10), 827-838 (2010).
73. Bach LA, Headey SJ, Norton RS. IGF-binding proteins--the pieces are falling into place. *Trends Endocrinol Metab* 16(5), 228-234 (2005).
74. Baxter RC. IGF binding proteins in cancer: mechanistic and clinical insights. *Nat Rev Cancer* 14(5), 329-341 (2014).
75. Kim HS, Nagalla SR, Oh Y, Wilson E, Roberts CT, Jr., Rosenfeld RG. Identification of a family of low-affinity insulin-like growth factor binding proteins (IGFBPs): characterization

of connective tissue growth factor as a member of the IGFBP superfamily. *Proc Natl Acad Sci U S A* 94(24), 12981-12986 (1997).
76. Kalus W, Zweckstetter M, Renner C *et al*. Structure of the IGF-binding domain of the insulin-like growth factor-binding protein-5 (IGFBP-5): implications for IGF and IGF-I receptor interactions. *EMBO J* 17(22), 6558-6572 (1998).
77. Bach LA. Insulin-like growth factor binding protein-6: the "forgotten" binding protein? *Horm Metab Res* 31(2-3), 226-234 (1999).
78. Bach LA. IGFBP-6 five years on; not so 'forgotten'? *Growth Horm IGF Res* 15(3), 185-192 (2005).
79. Bach LA. Recent insights into the actions of IGFBP-6. *J Cell Commun Signal* 9(2), 189-200 (2015).
80. Sitar T, Popowicz GM, Siwanowicz I, Huber R, Holak TA. Structural basis for the inhibition of insulin-like growth factors by insulin-like growth factor-binding proteins. *Proc Natl Acad Sci U S A* 103(35), 13028-13033 (2006).
81. Neumann GM, Bach LA. The N-terminal disulfide linkages of human insulin-like growth factor-binding protein-6 (hIGFBP-6) and hIGFBP-1 are different as determined by mass spectrometry. *J Biol Chem* 274(21), 14587-14594 (1999).
82. Chandrashekaran IR, Yao S, Wang CC *et al*. The N-terminal subdomain of insulin-like growth factor (IGF) binding protein 6. Structure and interaction with IGFs. *Biochemistry* 46(11), 3065-3074 (2007).
83. Headey SJ, Keizer DW, Yao S *et al*. C-terminal domain of insulin-like growth factor (IGF) binding protein-6: structure and interaction with IGF-II. *Mol Endocrinol* 18(11), 2740-2750 (2004).
84. Bach LA. Current ideas on the biology of IGFBP-6: More than an IGF-II inhibitor? *Growth Horm IGF Res* 30-31 81-86 (2016).
85. Shalamanova L, Kubler B, Storch S, Scharf JG, Braulke T. Multiple post-translational modifications of mouse insulin-like growth factor binding protein-6 expressed in epithelial Madin-Darby canine kidney cells. *Mol Cell Endocrinol* 295(1-2), 18-23 (2008).
86. Bach LA, Fu P, Yang Z. Insulin-like growth factor-binding protein-6 and cancer. *Clin Sci (Lond)* 124(4), 215-229 (2013).
87. Wang X, Lu L, Li Y *et al*. Molecular and functional characterization of two distinct IGF binding protein-6 genes in zebrafish. *Am J Physiol Regul Integr Comp Physiol* 5 1348-1357 (2009).
88. Hwa V, Oh Y, Rosenfeld RG. The insulin-like growth factor-binding protein (IGFBP) superfamily. *Endocr Rev* 20(6), 761-787 (1999).
89. Micutkova L, Diener T, Li C *et al*. Insulin-like growth factor binding protein-6 delays replicative senescence of human fibroblasts. *Mech Ageing Dev* 132(10), 468-479 (2011).
90. Fu P, Yang Z, Bach LA. Prohibitin-2 binding modulates insulin-like growth factor-binding protein-6 (IGFBP-6)-induced rhabdomyosarcoma cell migration. *J Biol Chem* 288(41), 29890-29900 (2013).
91. Bei Y, Huang Q, Shen J *et al*. IGFBP6 Regulates Cell Apoptosis and Migration in Glioma. *Cell Mol Neurobiol* 37(5), 889-898 (2017).
92. Chen Q, Qin S, Liu Y *et al*. IGFBP6 is a novel nasopharyngeal carcinoma prognostic biomarker. *Oncotarget* 7(42), 68140-68150 (2016).
93. Fell VL, Schild-Poulter C. The Ku heterodimer: function in DNA repair and beyond. *Mutat Res Rev Mutat Res* 763 15-29 (2015).
94. Iosef C, Vilk G, Gkourasas T *et al*. Insulin-like growth factor binding protein-6 (IGFBP-6) interacts with DNA-end binding protein Ku80 to regulate cell fate. *Cell Signal* 22(7), 1033-1043 (2010).
95. Maguschak KA, Ressler KJ. A role for WNT/beta-catenin signaling in the neural mechanisms of behavior. *J Neuroimmune Pharmacol* 7(4), 763-773 (2012).
96. Mulligan KA, Cheyette BN. Wnt signaling in vertebrate neural development and function. *J Neuroimmune Pharmacol* 7(4), 774-787 (2012).
97. Gao L, Chen B, Li J *et al*. Wnt/beta-catenin signaling pathway inhibits the proliferation and apoptosis of U87 glioma cells via different mechanisms. *PLoS One* 12(8), e0181346 (2017).
98. Denys H, Jadidizadeh A, Amini Nik S *et al*. Identification of IGFBP-6 as a significantly downregulated gene by beta-catenin in desmoid tumors. *Oncogene* 23(3), 654-664 (2004).
99. Mishra S, Ande SR, Nyomba BL. The role of prohibitin in cell signaling. *FEBS J* 277(19), 3937-3946 (2010).

100. Huang C, Jacobson K, Schaller MD. MAP kinases and cell migration. *J Cell Sci* 117(Pt 20), 4619-4628 (2004).
101. Qiu J, Ma XL, Wang X, Chen H, Huang BR. Insulin-like growth factor binding protein-6 interacts with the thyroid hormone receptor alpha1 and modulates the thyroid hormone-response in osteoblastic differentiation. *Mol Cell Biochem* 361(1-2), 197-208 (2012).
102. Pan H, Li X, Wang J *et al*. LIM Mineralization Protein-1 Enhances Bone Morphogenetic Protein-2-Mediated Osteogenesis Through Activation of ERK1/2 MAPK Pathway and Upregulation of Runx2 Transactivity. *J Bone Miner Res* 30(8), 1523-1535 (2015).
103. Strohbach C, Kleinman S, Linkhart T *et al*. Potential involvement of the interaction between insulin-like growth factor binding protein (IGFBP)-6 and LIM mineralization protein (LMP)-1 in regulating osteoblast differentiation. *J Cell Biochem* 104(5), 1890-1905 (2008).
104. Cui J, Ma C, Qiu J *et al*. A novel interaction between insulin-like growth factor binding protein-6 and the vitamin D receptor inhibits the role of vitamin D3 in osteoblast differentiation. *Mol Cell Endocrinol* 338(1-2), 84-92 (2011).
105. Seurin D, Lassarre C, Bienvenu G, Babajko S. Insulin-like growth factor binding protein-6 inhibits neuroblastoma cell proliferation and tumour development. *Eur J Cancer* 38(15), 2058-2065 (2002).
106. Leng SL, Leeding KS, Whitehead RH, Bach LA. Insulin-like growth factor (IGF)-binding protein-6 inhibits IGF-II-induced but not basal proliferation and adhesion of LIM 1215 colon cancer cells. *Mol Cell Endocrinol* 174(1-2), 121-127 (2001).
107. Yang Z, Bach LA. Differential Effects of Insulin-Like Growth Factor Binding Protein-6 (IGFBP-6) on Migration of Two Ovarian Cancer Cell Lines. *Front Endocrinol (Lausanne)* 5 231 (2014).
108. Koike H, Ito K, Takezawa Y, Oyama T, Yamanaka H, Suzuki K. Insulin-like growth factor binding protein-6 inhibits prostate cancer cell proliferation: implication for anticancer effect of diethylstilbestrol in hormone refractory prostate cancer. *Br J Cancer* 92(8), 1538-1544 (2005).
109. Gallicchio MA, Kneen M, Hall C, Scott AM, Bach LA. Overexpression of insulin-like growth factor binding protein-6 inhibits rhabdomyosarcoma growth in vivo. *Int J Cancer* 94(5), 645-651 (2001).
110. Visser M, Sijmons C, Bras J *et al*. Allelotype of pediatric rhabdomyosarcoma. *Oncogene* 15(11), 1309-1314 (1997).
111. Barr FG. Gene fusions involving PAX and FOX family members in alveolar rhabdomyosarcoma. *Oncogene* 20(40), 5736-5746 (2001).
112. Pollak MN. Insulin-like growth factors and neoplasia. *Novartis Found Symp* 262 84-98; discussion 98-107, 265-108 (2004).
113. Wang W, Slevin M, Kumar S, Kumar P. The cooperative transforming effects of PAX3-FKHR and IGF-II on mouse myoblasts. *Int J Oncol* 27(4), 1087-1096 (2005).
114. Toretsky JA, Helman LJ. Involvement of IGF-II in human cancer. *J Endocrinol* 149(3), 367-372 (1996).
115. Foulstone E, Prince S, Zaccheo O *et al*. Insulin-like growth factor ligands, receptors, and binding proteins in cancer. *J Pathol* 205(2), 145-153 (2005).
116. Fu P, Liang GJ, Khot SS, Phan R, Bach LA. Cross-talk between MAP kinase pathways is involved in IGF-independent, IGFBP-6-induced Rh30 rhabdomyosarcoma cell migration. *J Cell Physiol* 224(3), 636-643 (2010).
117. Fu P, Thompson JA, Bach LA. Promotion of cancer cell migration: an insulin-like growth factor (IGF)-independent action of IGF-binding protein-6. *J Biol Chem* 282(31), 22298-22306 (2007).
118. Wu L, Li C, Pan L. Nasopharyngeal carcinoma: A review of current updates. *Exp Ther Med* 15(4), 3687-3692 (2018).
119. Wildeman MA, Fles R, Herdini C *et al*. Primary treatment results of Nasopharyngeal Carcinoma (NPC) in Yogyakarta, Indonesia. *PLoS One* 8(5), e63706 (2013).
120. Hirayama T. Descriptive and analytical epidemiology of nasopharyngeal cancer. *IARC Sci Publ* (20), 167-189 (1978).
121. Zhang LF, Li YH, Xie SH *et al*. Incidence trend of nasopharyngeal carcinoma from 1987 to 2011 in Sihui County, Guangdong Province, South China: an age-period-cohort analysis. *Chin J Cancer* 34(8), 350-357 (2015).
122. Sarmiento MP, Mejia MB. Preliminary assessment of nasopharyngeal carcinoma incidence in the Philippines: a second look at published data from four centers. *Chin J Cancer* 33(3), 159-164 (2014).

123. Brennan B. Nasopharyngeal carcinoma. *Orphanet J Rare Dis* 1 23 (2006).
124. Lo KW, To KF, Huang DP. Focus on nasopharyngeal carcinoma. *Cancer Cell* 5(5), 423-428 (2004).
125. Tang LQ, Li CF, Li J *et al*. Establishment and Validation of Prognostic Nomograms for Endemic Nasopharyngeal Carcinoma. *J Natl Cancer Inst* 108(1), (2016).
126. Fung LF, Lo AK, Yuen PW, Liu Y, Wang XH, Tsao SW. Differential gene expression in nasopharyngeal carcinoma cells. *Life Sci* 67(8), 923-936 (2000).
127. Kuo YS, Tang YB, Lu TY, Wu HC, Lin CT. IGFBP-6 plays a role as an oncosuppressor gene in NPC pathogenesis through regulating EGR-1 expression. *J Pathol* 222(3), 299-309 (2010).
128. Sandberg AC, Engberg C, Lake M, Von Holst H, Sara VR. The expression of insulin-like growth factor I and insulin-like growth factor II genes in the human fetal and adult brain and in glioma. *Neurosci Lett* 93(1), 114-119 (1988).
129. Livingstone C. IGF2 and cancer. *Endocr Relat Cancer* 20(6), R321-339 (2013).
130. Maris C, D'haene N, Trepant AL *et al*. IGF-IR: a new prognostic biomarker for human glioblastoma. *Br J Cancer* 113(5), 729-737 (2015).
131. Oliva CR, Halloran B, Hjelmeland AB *et al*. IGFBP6 controls the expansion of chemoresistant glioblastoma through paracrine IGF2/IGF-1R signaling. *Cell Commun Signal* 16(1), 61 (2018).
132. Freije WA, Castro-Vargas FE, Fang Z *et al*. Gene expression profiling of gliomas strongly predicts survival. *Cancer Res* 64(18), 6503-6510 (2004).
133. Lin Y, Zhang G, Zhang J *et al*. A panel of four cytokines predicts the prognosis of patients with malignant gliomas. *J Neurooncol* 114(2), 199-208 (2013).
134. Pazaitou-Panayiotou K, Kelesidis T, Kelesidis I *et al*. Growth hormone-binding protein is directly and IGFBP-3 is inversely associated with risk of female breast cancer. *Eur J Endocrinol* 156(2), 187-194 (2007).
135. Denduluri SK, Idowu O, Wang Z *et al*. Insulin-like growth factor (IGF) signaling in tumorigenesis and the development of cancer drug resistance. *Genes Dis* 2(1), 13-25 (2015).
136. Lu Y, Zi X, Zhao Y, Mascarenhas D, Pollak M. Insulin-like growth factor-I receptor signaling and resistance to trastuzumab (Herceptin). *J Natl Cancer Inst* 93(24), 1852-1857 (2001).
137. Ye XM, Zhu HY, Bai WD *et al*. Epigenetic silencing of miR-375 induces trastuzumab resistance in HER2-positive breast cancer by targeting IGF1R. *BMC Cancer* 14 134 (2014).
138. Oliveras-Ferraros C, Vazquez-Martin A, Martin-Castillo B *et al*. Pathway-focused proteomic signatures in HER2-overexpressing breast cancer with a basal-like phenotype: new insights into de novo resistance to trastuzumab (Herceptin). *Int J Oncol* 37(3), 669-678 (2010).
139. Kaulsay KK, Ng EH, Ji CY, Ho GH, Aw TC, Lee KO. Serum IGF-binding protein-6 and prostate specific antigen in breast cancer. *Eur J Endocrinol* 140(2), 164-168 (1999).
140. Vargas AN. Natural history of ovarian cancer. *Ecancermedicalscience* 8 465 (2014).
141. Doubeni CA, Doubeni AR, Myers AE. Diagnosis and Management of Ovarian Cancer. *Am Fam Physician* 93(11), 937-944 (2016).
142. Sayer RA, Lancaster JM, Pittman J *et al*. High insulin-like growth factor-2 (IGF-2) gene expression is an independent predictor of poor survival for patients with advanced stage serous epithelial ovarian cancer. *Gynecol Oncol* 96(2), 355-361 (2005).
143. Walker G, Macleod K, Williams AR, Cameron DA, Smyth JF, Langdon SP. Insulin-like growth factor binding proteins IGFBP3, IGFBP4, and IGFBP5 predict endocrine responsiveness in patients with ovarian cancer. *Clin Cancer Res* 13(5), 1438-1444 (2007).
144. Paschou SA, Papadopoulou-Marketou N, Chrousos GP, Kanaka-Gantenbein C. On type 1 diabetes mellitus pathogenesis. *Endocr Connect* 7(1), R38-R46 (2018).
145. Itariu BK, Stulnig TM. Autoimmune aspects of type 2 diabetes mellitus - a mini-review. *Gerontology* 60(3), 189-196 (2014).
146. Feldmann B, Jehle PM, Mohan S *et al*. Diabetic retinopathy is associated with decreased serum levels of free IGF-I and changes of IGF-binding proteins. *Growth Horm IGF Res* 10(1), 53-59 (2000).
147. Lu S, Purohit S, Sharma A *et al*. Serum insulin-like growth factor binding protein 6 (IGFBP6) is increased in patients with type 1 diabetes and its complications. *Int J Clin Exp Med* 5(3), 229-237 (2012).
148. Han X, Hou S, Yang A. Correlation Between IGFs-Related Proteins Expression and Incidence of Colorectal Cancer in Diabetic Patients and Related Mechanisms. *Med Sci Monit* 22 848-854 (2016).

149. Matsumoto T, Yamashita S, Rosenfeld RG. Increased levels of IGF-I and IGFBP-3 in synovial fluids of patients with rheumatoid arthritis. *Endocr J* 45 Suppl S141-144 (1998).
150. Tavera C, Abribat T, Reboul P *et al*. IGF and IGF-binding protein system in the synovial fluid of osteoarthritic and rheumatoid arthritic patients. *Osteoarthritis Cartilage* 4(4), 263-274 (1996).
151. Fernihough JK, Billingham ME, Cwyfan-Hughes S, Holly JM. Local disruption of the insulin-like growth factor system in the arthritic joint. *Arthritis Rheum* 39(9), 1556-1565 (1996).
152. Matsumoto T, Gargosky SE, Iwasaki K, Rosenfeld RG. Identification and characterization of insulin-like growth factors (IGFs), IGF-binding proteins (IGFBPs), and IGFBP proteases in human synovial fluid. *J Clin Endocrinol Metab* 81(1), 150-155 (1996).
153. Alunno A, Bistoni O, Manetti M *et al*. Insulin-Like Growth Factor Binding Protein 6 in Rheumatoid Arthritis: A Possible Novel Chemotactic Factor? *Front Immunol* 8 554 (2017).
154. Irizarry RA, Bolstad BM, Collin F, Cope LM, Hobbs B, Speed TP. Summaries of Affymetrix GeneChip probe level data. *Nucleic Acids Res* 31(4), e15 (2003).
155. Fisher RA. On the interpretation of $\chi 2$ from contingency tables, and the calculation of P. *Journal of the Royal Statistical Society* 85 87-94 (1922).
156. Reiner A, Yekutieli D, Benjamini Y. Identifying differentially expressed genes using false discovery rate controlling procedures. *Bioinformatics* 19(3), 368-375 (2003).
157. Klink M, Tchorzewski H, Sulowska Z. Oxidative and adhesive responses of human neutrophils to nitrovasodilators in vitro: the role of protein kinases. *Mediators Inflamm* 12(6), 345-353 (2003).
158. Capuozzo E, Baseggio Conrado A, Fontana M. Thiotaurine modulates human neutrophil activation. *Adv Exp Med Biol* 803 145-155 (2015).
159. Castellani S, Guerra L, Favia M, Di Gioia S, Casavola V, Conese M. NHERF1 and CFTR restore tight junction organisation and function in cystic fibrosis airway epithelial cells: role of ezrin and the RhoA/ROCK pathway. *Lab Invest* 92(11), 1527-1540 (2012).
160. Edens HA, Levi BP, Jaye DL *et al*. Neutrophil transepithelial migration: evidence for sequential, contact-dependent signaling events and enhanced paracellular permeability independent of transjunctional migration. *J Immunol* 169(1), 476-486 (2002).
161. Lindholm P, Peranen J, Andressoo JO *et al*. MANF is widely expressed in mammalian tissues and differently regulated after ischemic and epileptic insults in rodent brain. *Mol Cell Neurosci* 39(3), 356-371 (2008).
162. Apostolou A, Shen Y, Liang Y, Luo J, Fang S. Armet, a UPR-upregulated protein, inhibits cell proliferation and ER stress-induced cell death. *Exp Cell Res* 314(13), 2454-2467 (2008).
163. Kim Y, Park SJ, Chen YM. Mesencephalic astrocyte-derived neurotrophic factor (MANF), a new player in endoplasmic reticulum diseases: structure, biology, and therapeutic roles. *Transl Res* 188 1-9 (2017).
164. Castellino FJ, Ploplis VA. Structure and function of the plasminogen/plasmin system. *Thromb Haemost* 93(4), 647-654 (2005).
165. Ladenvall P, Nilsson S, Jood K, Rosengren A, Blomstrand C, Jern C. Genetic variation at the human tissue-type plasminogen activator (tPA) locus: haplotypes and analysis of association to plasma levels of tPA. *Eur J Hum Genet* 11(8), 603-610 (2003).
166. Babu PV, Si H, Fu Z, Zhen W, Liu D. Genistein prevents hyperglycemia-induced monocyte adhesion to human aortic endothelial cells through preservation of the cAMP signaling pathway and ameliorates vascular inflammation in obese diabetic mice. *J Nutr* 142(4), 724-730 (2012).
167. Landriscina M, Altamura SA, Roca L *et al*. Reverse transcriptase inhibitors induce cell differentiation and enhance the immunogenic phenotype in human renal clear-cell carcinoma. *Int J Cancer* 122(12), 2842-2850 (2008).
168. Verhasselt V, Goldman M, Willems F. Oxidative stress up-regulates IL-8 and TNF-alpha synthesis by human dendritic cells. *Eur J Immunol* 28(11), 3886-3890 (1998).
169. Guerra L, D'oria S, Favia M *et al*. CFTR-dependent chloride efflux in cystic fibrosis mononuclear cells is increased by ivacaftor therapy. *Pediatr Pulmonol* 52(7), 900-908 (2017).
170. Papac RJ. Spontaneous regression of cancer. *Cancer Treat Rev* 22(6), 395-423 (1996).
171. Hobohm U. Fever and cancer in perspective. *Cancer Immunol Immunother* 50(8), 391-396 (2001).
172. Wust P, Hildebrandt B, Sreenivasa G *et al*. Hyperthermia in combined treatment of cancer. *Lancet Oncol* 3(8), 487-497 (2002).

173. Saga T, Sakahara H, Nakamoto Y *et al*. Enhancement of the therapeutic outcome of radio-immunotherapy by combination with whole-body mild hyperthermia. *Eur J Cancer* 37(11), 1429-1434 (2001).
174. Li DY, Gu C, Min J, Chu ZH, Ou QJ. Maturation induction of human peripheral blood mononuclear cell-derived dendritic cells. *Exp Ther Med* 4(1), 131-134 (2012).
175. Jaattela M. Heat shock proteins as cellular lifeguards. *Ann Med* 31(4), 261-271 (1999).
176. Punyiczki M, Fesus L. Heat shock and apoptosis. The two defense systems of the organism may have overlapping molecular elements. *Ann N Y Acad Sci* 851 67-74 (1998).
177. Hasday JD, Singh IS. Fever and the heat shock response: distinct, partially overlapping processes. *Cell Stress Chaperones* 5(5), 471-480 (2000).
178. Tsan MF, Gao B. Heat shock proteins and immune system. *J Leukoc Biol* 85(6), 905-910 (2009).
179. Zininga T, Ramatsui L, Shonhai A. Heat Shock Proteins as Immunomodulants. *Molecules* 23(11), (2018).
180. Calderwood SK, Gong J, Murshid A. Extracellular HSPs: The Complicated Roles of Extracellular HSPs in Immunity. *Front Immunol* 7 159 (2016).
181. Juwono J, Martinus RD. Does Hsp60 Provide a Link between Mitochondrial Stress and Inflammation in Diabetes Mellitus? *J Diabetes Res* 2016 8017571 (2016).
182. Borges TJ, Wieten L, Van Herwijnen MJ *et al*. The anti-inflammatory mechanisms of Hsp70. *Front Immunol* 3 95 (2012).
183. Gross C, Schmidt-Wolf IG, Nagaraj S *et al*. Heat shock protein 70-reactivity is associated with increased cell surface density of CD94/CD56 on primary natural killer cells. *Cell Stress Chaperones* 8(4), 348-360 (2003).
184. Mbofung RM, Mckenzie JA, Malu S *et al*. HSP90 inhibition enhances cancer immunotherapy by upregulating interferon response genes. *Nat Commun* 8(1), 451 (2017).
185. Mitra S, Abraham E. Participation of superoxide in neutrophil activation and cytokine production. *Biochim Biophys Acta* 1762(8), 732-741 (2006).
186. Faurschou M, Borregaard N. Neutrophil granules and secretory vesicles in inflammation. *Microbes Infect* 5(14), 1317-1327 (2003).